The interactions of elementary particles in nuclear emulsions

Finny, Peter John

The Interactions of Elementary Particles in Nuclear Emulsions

A thesis presented by

Peter John Finney

for the

Degree of Doctor of Philosophy

at the

University of Durham

October 1963

CONTENTS

P R E F A C E

This thesis is an account of some of the work carried out by the author whilst at Durham University. It is concerned with the interactions of negative π-mesons at 16.3 GeV and the search for "Ferretti Tridents". The exposure to the 16.3 GeV negative π-meson beam was carried out by the CERN Emulsion Group. The experiment was carried out with the collaboration of Dr. J. V. Major and Dr. A. J. Apostolakis. The measurements were made with the assistance of Miss M. G. Welton and Mr. M. E. Williams. The analysis of the results presented in this thesis has been the sole responsibility of the author.

The earlier work, on the interactions of 300 MeV negative π-mesons carried out by the author with the collaboration of Dr. J. V. Major and Mr. P. G. J. T. Parkhouse, is not included here.

LIST OF FIGURES

LIST OF TABLES

INTRODUCTION

The study of nuclear interactions produced by high energy cosmic rays has led to a number of theories on multi-meson production in collisions between a primary particle and a target nucleon. In such collisions the energy of the primary particle is not known nor can it be measured directly. Consequently methods, such as the Castagnoli formula, have been devised to estimate the primary energy from the angular distribution of the secondary particles. Basically this method determines the velocity of the centre of mass of the interactingsystem and assuming that the target is a single nucleon the primary energy can be estimated.

The advent of high energy accelerators has made it possible to produce beams of known particles of known high energy. With these it is possible to check the method of estimating the primary energy from the angular distribution of the secondary particles and to test the predictions of some of the theories.

Most of the work on high energy meson production has been carried out with the emulsion technique. Consequently the observed interactions have resulted from collisions between the primary particles and the complex nuclei of the emulsion. The basic interaction inside the nucleus will be with single nucleons or groups of nucleons and may be followed by secondary interactions

within the same nucleus. It is necessary to devise methods whereby those interactions involving only one collision can be selected. Then the characteristics of meson production can be investigated.

If the primary energy is known the application of the Castagnoli formula to the secondary particles leads finally to an estimate of the masse of the struck target particle. This type of analysis has been carried out by Friedlander (1960) with 7.3 GeV negative π-mesons. His analysis yields a spectrum of target masses with peaks corresponding to one and two nucleon and one, two and three π-meson masses.

The Castagnoli formula has been applied to interactions, at machine energies, with complex nuclei on the assumption thatthe target is always a single nucleon in contrast to Friedlander's results.

In the above work no allowance has been made for secondary interactions.

In this thesis the interactions of 16 GeV negative π-mesons have been investigated. It has not been possible to confirm the observations of Friedlander. It is found that there are two classes of interaction, both involving a collision with a single nucleon but in one group this is followed by secondary collisions. For the former group the Castagnoli formula is found to hold for all star sizes subject to a correction allowing for the misclassification of the continuing primary as a secondary meson.

In Chapter 1 a summary of the methods of determining the energy of primary particles from the angular distribution of secondary particles is given. The various models of multi-meson production are described and these are followed by some results on the application of the methods for determining the energies of primary particles. The chapter is concluded with a discussion of difficulties encountered when applying these methods.

In Chapter 2 the general results of the interactions of 16.3 GeV π^--mesons are given and this is followed by a comparison of the experimentally determined values of the primary energy with the known value. The observed discrepancies are then discussed. Chapter 3 shows how it is possible to account for the discrepancies in Chapter 2 in terms of secondary interactions in the complex nuclei and the continuing primary. This chapter includes a detailed analysis of the secondary interactions.

Chapter 4 deals with the pair production of π-mesons in the Coulomb and nuclear fields of nuclei.

Further work in these laboratories has been concerned with the interactions of 25 GeV protons inemulsion. The methods of analysis devised in this thesis have been applied successfully there.

CHAPTER 1

Determination of the Primary Energy in High Energy Interactions

Two methods of estimating the energy of the primary particles in very high energy interactions, which have been developed by Castagnoli (1953) and Duller and Walker (1954), are discussed in sections 1.1 and 1.2. These methods depend on the angular distribution of the secondary particles produced in the interactions.

1.1 The Castagnoli Formula

This formula is based on three assumptions which are:-

(i) The interaction is due to a nucleon-nucleon collision.

(ii) The angular distribution of all the shower particles emitted in the interaction or jet is symmetrical with respect to the equatorial plane in the centre of mass system.

(iii) The shower particles are independent in the sense that there is no correlation between their angles or between their energies of emission.

The formula can be applied by successive approximations. In the first approximation the assumption is made that all the emitted particles have the same velocity as the two colliding nucleons in the centre of mass system i.e. $\beta^{x} = \beta_{c}$.

The second approximation takes into account the energy spectrum of the produced particles and needs the introduction of some special assumptions.

Consider the transformation of the angles from the centre of mass system to the laboratory system.

$$\gamma_c = \frac{1}{|\tan\theta|} \cdot \frac{(1-\cos^2\theta^*)^{\frac{1}{2}}}{(z + \cos\theta^*)} \qquad \ldots\ldots 1$$

θ is the angle of the shower particle relative to the primary particle in the laboratory system and θ^x the corresponding angle in the centre of mass system. Z is the ratio $\frac{\beta_c}{\beta^x}$ and γ_c is given by $(1 - \beta_c^2)^{-\frac{1}{2}}$.

The equation 1 is usually used in the form

$$\ell n\ \gamma_c = \ell n|\cot\theta| + \ell n \left\{\frac{(1-\cos^2\theta^*)^{\frac{1}{2}}}{(z + \cos\theta^*)}\right\} \qquad \ldots\ldots 2$$

Since each track can be treated independently to obtain a value of γ_c, equation 2 can be applied to all tracks and taking the sum of all values it follows that

$$\ell n\ \gamma_c = \frac{1}{n_s} \cdot \sum_{i=1}^{n_s} \ell n|\cot\theta_i| + \frac{1}{n_s} \sum_{i=1}^{n_s} \ell n \left\{\frac{(1-\cos^2\theta^*)^{\frac{1}{2}}}{(z + \cos\theta^*)}\right\} \ldots\ldots 3$$

The first term of the right hand side of equation 3 contains the results of the angular measurements, while the second term contains unknowns which depend on the energy and angular distribution of the emitted particles in the centre of mass system.

Equation 3 can be used to determine γ_c from experimental angular distributions if the second term can be evaluated. From the assump-

tion $\beta^x = \beta_c$ of the first approximation it follows that Z = 1 and consequently the second term of equation 3 becomes

$$x = \ell n \left\{ \frac{(1 - \cos^2\theta^*)^{1/2}}{(1 + \cos\theta^*)} \right\} = \ell n \tan \theta^*/2 \qquad \ldots\ldots 4$$

On the assumption that the angular distribution in the centre of mass system is symmetrical, it follows that the probability of x having a value between x and x+dx, f(x)dx, is an even function of x. Therefore the average value of x is given by

$$\bar{x} = \int_{-\infty}^{+\infty} x f(x)dx = 0 \qquad \ldots\ldots 5$$

for large n_s.

Equation 2 can be written

$$\ell n\, \gamma_c - \ell n|\cot\theta_i| = x_i \qquad \ldots\ldots 6$$

and can be interpreted by saying that the variable x_i fluctuates about the average value of eqn. 5, with a variance given by

$$\sigma^2 = \overline{x^2} = \int_{-\infty}^{+\infty} x^2 f(x)dx \qquad \ldots\ldots 7$$

Thus if the emitted particles are independent (assumption (iii)), and using equations 3, 5 and 7, $\ell n\, \gamma_c$ is given by

$$\ell n\, \gamma_c = \frac{1}{n_s} \sum_{i=1}^{n_s} \ell n|\cot\theta_i| \pm \frac{\sigma_o}{\sqrt{n_s}} \qquad \ldots\ldots 8$$

σ_o has been calculated by Castagnoli for an isotropic angular distribution in the centre of mass system and is 0.906.

In the case of the second approximation the second term of equation 3 is evaluated. The assumption $\beta_c/\beta^* = Z = 1$ is not made and the range of values of Z can be estimated using one of the theoretical models of Fermi or Heisenberg. These models also give the angular distribution of the secondary particles in the centre of mass system and hence it is possible to evaluate the second term for each model. However, previous experimental work has been analysed using the first approximation and consequently the present work has been similarly analysed. Moreover, it will be shown that the first approximation leads to a result which is in good agreement with the known value of γ_c.

1.2 The Duller and Walker Plot

This method of displaying the angular distribution of the shower particles in a jet produced in a N-N collision takes as its starting point the same transformation 1 as used in the Castagnoli formula but expressed slightly differently

$$\tan \theta = \frac{1}{\gamma_c} \frac{\sin \theta^*}{(Z + \cos \theta^*)} \qquad \ldots\ldots 9$$

where the variables are denoted as in equation 1. For an isotropic angular distribution of emitted particles in the centre of mass system, the fraction of particles emitted with angles up to θ^x is given by

$$F = \sin^2 \frac{\theta^*}{2} \qquad \ldots\ldots 10$$

Making the assumption Z = 1, equation 9 can be written

$$\tan \theta = \frac{1}{\gamma_c} \frac{\sin \theta^*/2}{\cos \theta^*/2} \qquad \ldots\ldots 11$$

Taking logarithms of the square of this equation and using equation 10 the equation,

$$2 \ell n \tan \theta = \ell n \left(\frac{1}{\gamma_c^2} \cdot \frac{\sin^2 \theta^*/2}{\cos^2 \theta^*/2} \right) = \ell n \left(\frac{F(\theta)}{1-F(\theta)} \cdot \frac{1}{\gamma_c^2} \right) \ldots 12$$

is obtained.

This equation represents a line of slope 2 passing through the point $F(\theta)/1-F(\theta) = \gamma_c^2$ at $\tan \theta = 1$.

Both the Castagnoli formula and the Duller and Walker plot were initially verified to some extent with cosmic ray data on nucleon interactions in nuclei. (Castagnoli 1953, Duller and Walker 1954). In each case care was taken to select those events which probably correspond to nucleon-nucleon collisions.

1.3 Models of Multi-meson Production

The Castagnoli Formula and the Duller and Walker Plot have been used in the analysis of very high energy cosmic ray interactions observed in nuclear emulsions, (Ciok et al. 1957 and 1958, Gierula et al. 1960a, b and c).

From this work two groups of interactions have been observed. For nucleon-nucleon interactions at energies up to about 100 GeV the analysis indicates that the angular distribution is isotropic

in the centre of mass of the colliding nucleons. For interactions at energies greater than 100 GeV the angular distribution in the centre of mass is anisotropic but symmetric.

The first group of interactions has been interpreted as due to the production of mesons from one excited centre. This centre is travelling with the velocity of the centre of mass, and is possibly an excited compound state of the two interacting particles.

Several authors have produced theories of multiple meson production in order to explain the anisotropic angular distribution of particles produced in very high energy interactions i.e. >100 GeV. All the theories are based on the assumption that the created mesons are emitted independently from two centres moving in opposite directions in the centre of mass system.

Takagi (1952) assumed that the secondary particles are emitted isotropically in the frames of reference associated with each centre. This results in the particles being concentrated in the forward and backward directions in the centre of mass system.

Kraushaar and Marks (1954) suggested a similar model in which the two centres are assumed to be highly excited nucleons.

Further studies by Ciok et al. 1958 have shown that for very high energy interactions the values of γ for the emitting centres, in the centre of mass system, are much smaller than the corresponding values of γ for the nucleons. This rules out the possibility that the two emitting centres are excited nucleons.

Heisenberg (1952) and Landau and Belenky (1956) have produced theories which predict an anisotropic angular distribution in the centre of mass which leads to lines of slope 1 on the Duller and Walker Plot. These distributions do not agree with the data for very high energy collisions. The best fit to the experimental data is given by the two centre model of Takagi.

It is possible to interpret nucleon-nucleon interactions at energies less than 100 GeV in terms of the two centre model also. If the distribution of $\ell n|\cot\theta|$ for each track is plotted then the distribution should comprise the separate distributions of $\ell n|\cot\theta|$ for the two centres. These will consist of gaussian distributions with a standard deviation of $\sigma_0 = 0.906$ centred at the values of $\ell n\gamma$, for the two centres. The distributions overlap and may not be distinguishable from a gaussian distribution which is distributed about the value of $\ell n\gamma$ for the centre of mass system of the colliding nucleons. However if these centres are separated by 1.07 then the two distributions should be resolved. The standard deviation of the total distribution will be $1.54\sigma_0$.

Although the foregoing calculations have been based on a nucleon-nucleon interaction, the formulae derived are quite general and will hold for the interaction between a π-meson and a nucleon.

1.4 The application of the Castagnoli Formula and Duller and Walker Plot

The first detailed investigation using the type of analysis

described in section 1.1 and 1.2 has been carried out by Friedlander (1960) using a beam of 7.3 GeV negative π-mesons. Friedlander shows that using the Castagnoli formula it should be possible to distinguish individual target masses of π, 2π, N, 2N etc. The differences between $\ell n\ \gamma_c$ for collisions of 7.3 GeV π^--mesons with these target masses are approximately 0.46 whereas the distribution of the experimental values for each target mass has a width which is expected to be about 0.45 for an average multiplicity of 4. The distribution of $\ell n\ \gamma_c$ for all interactions should therefore show a series of overlapping gaussians with maxima at values of $\ell n\ \gamma_c$ corresponding to collisions between π^--mesons and target masses of π, 2π, N and 2N.

The distributions of $\ell n\ \gamma_c$ for interactions in heavy and light nuclei given by Friedlander (figures 1 and 2) show some correlation with the expected values of $\ell n\ \gamma_c$. Furthermore, when the events are classified according to the range of $\ell n\ \gamma_c$ and the Duller and Walker diagrams are constructed, the experimental results indicate that the emitted particles have an isotropic angular distribution in the centre of mass system for collisions with one and two nucleons. Collisions between one and two π-mesons have a symmetric but anisotropic distribution, which is similar to the two centre effect discussed in section 1.3.

However, in Friedlander's work events are considered with n_h ranging from 1 to 4 and no allowance has been made for the possible effect of secondary collisions in heavy nuclei.

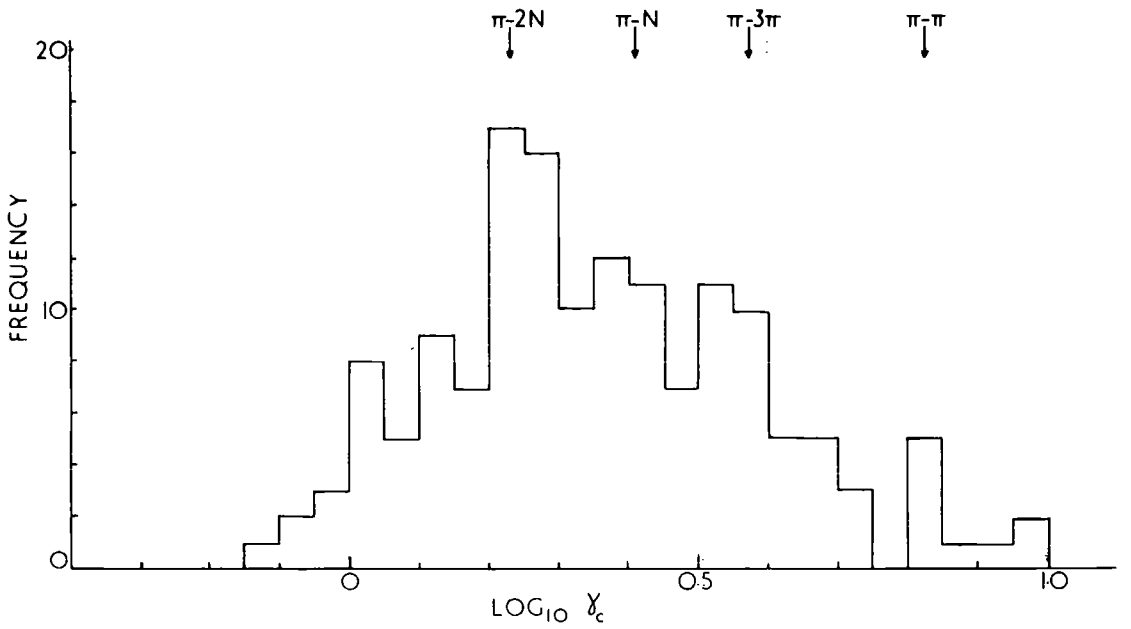

Fig.1. The distribution of $\log_{10} \gamma_c$ for events with $n_h \leqslant 4$ produced by 7·3 GeV. π^--mesons (Friedlander 1960)

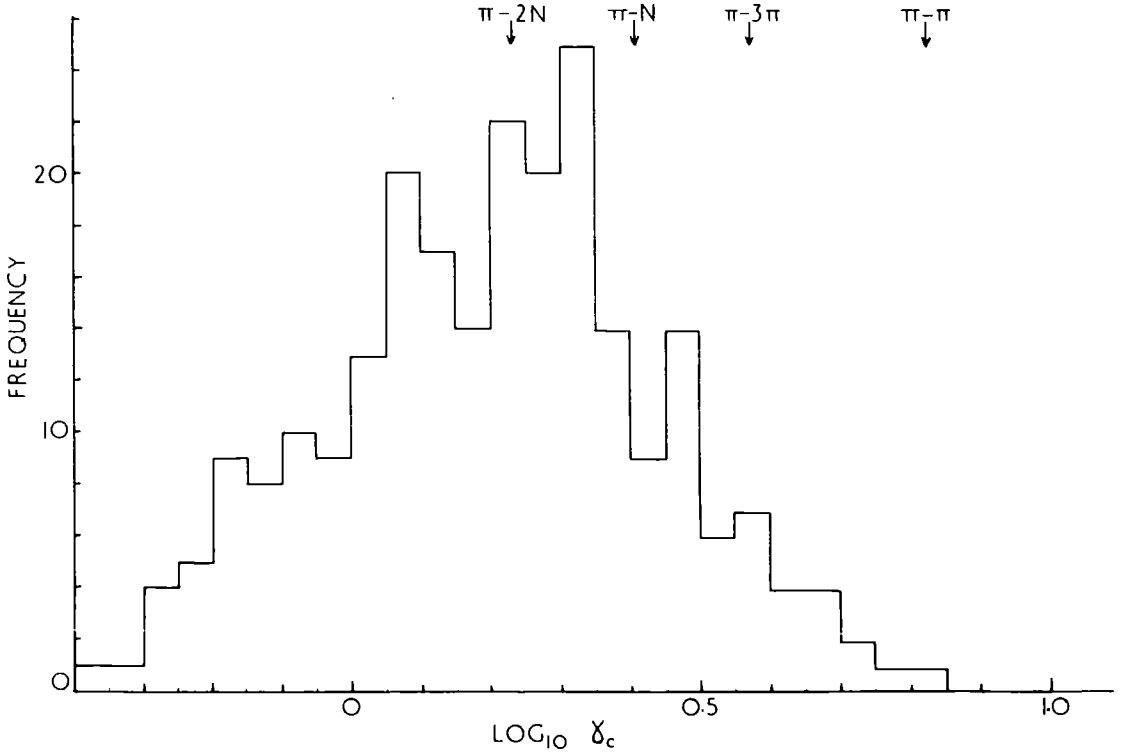

Fig. 2. The distribution of $\log_{10} \gamma_c$ for events with $n_h > 4$ produced by 7·3 GeV. π^- - mesons (Friedlander 1960)

1.5 Difficulties involved in the application of the Castagnoli Formula and Duller and Walker Plot

1.51 Secondary Collisions

The use of nuclear emulsions leads to the observation of interactions of π-mesons with complex nuclei resulting from several collisions within nuclei by the primary and secondary particles.

Figure 3 shows the variation of multiplicity with energy for the interaction of π-mesons and protons with nucleons and nuclei. For energies below approximately 8 GeV it can be seen that the multiplicity for the interactions of π-mesons and protons with nuclei is less than that for interactions with single nucleons. For energies above 8 GeV the reverse is the case.

This effect can be interpreted in terms of secondary collisions. For interactions in the energy range up to 8 GeV the average energy of the secondary particles is too low to lead to further production in a secondary collision. In fact the secondary mesons of lower energy will tend to be absorbed, leading to a lower multiplicity for interactions with nuclei than with nucleons.

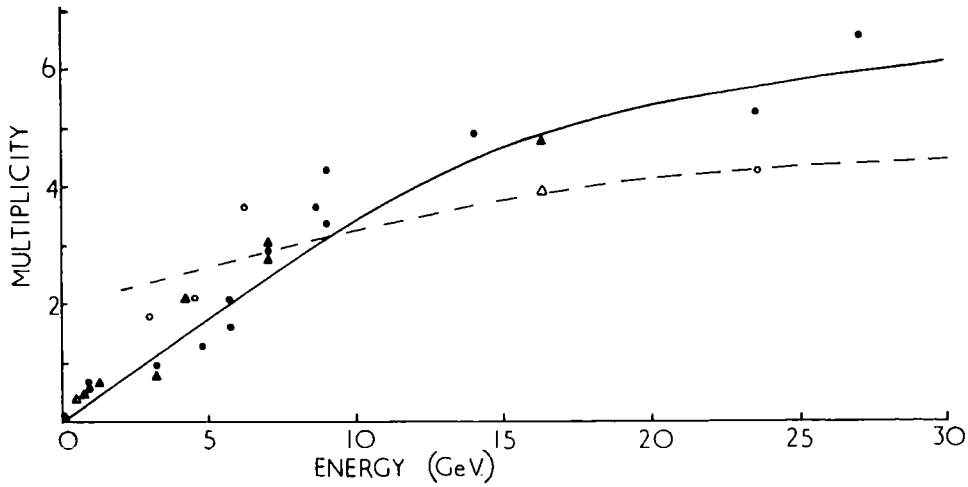

Fig. 3. The variation of multiplicity with energy for p–p, ∘; p–nucleus, •; π–p, △; and π–nucleus, ▲; collisions
——— collisions with nuclei
– – – – collisions with nucleons

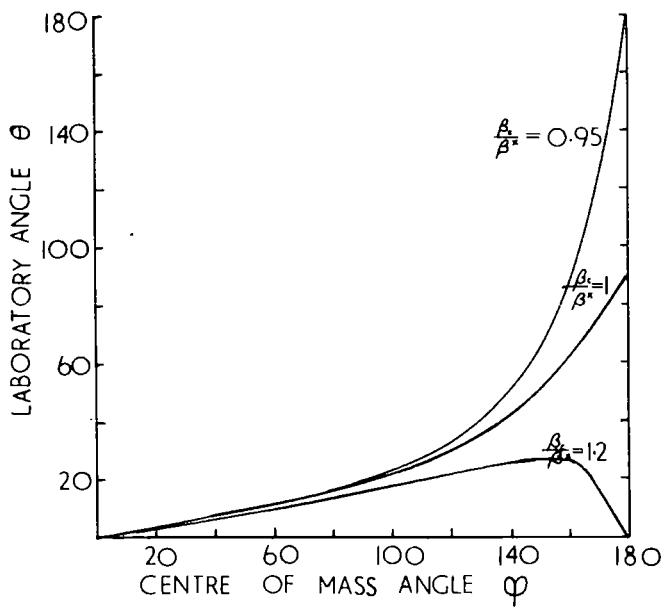

Fig. 4. The relation between the of angle of emission in the centre of mass and laboratory systems for secondary particles whose velocities are given by $\frac{\beta_1}{\beta^*}=0.95$, 1 and 1.2

Above 8 GeV the energies of the secondary particles are somewhat higher, and if secondary collisions occur further production of π-mesons is likely to take place, leading to a higher multiplicity in the case of interactions with nuclei than with the interactions with nucleons.

At 16 GeV secondary collisions lead to further production of π-mesons and consequently to a broadening of the angular distribution of shower particles which results in a low value of $\overline{\ell n|\cot\theta|}$. In the analysis of Friedlander this would be interpreted as an interaction between the incident particle and a target heavier than a nucleon.

1.52 Continuing Primary

According to Menon (private communication) the cross-section for charge exchange of 16 GeV π^--mesons is negligible. Consequently in their interaction the primary π^--mesons will emerge and will be classified experimentally as shower particles.

Moreover the continuing primary is likely to be highly collimated in the laboratory system. If it is classified as a secondary particle its value of $\ell n|\cot\theta|$ will be large and it will lead to an abnormally large value of $\ell n\ \gamma_c$ particularly for small values of n_s. Again, in the analysis of Friedlander, this would be interpreted as an interaction between the incident π-meson and some target mass which is smaller than that of a nucleon. The effect of the contin-

uing primary will become progressivly smaller as the value of n_s increases.

1.53 Distribution of Velocities in the Centre of Mass System

In the application of both the Castagnoli Formula and the Duller and Walker plot the assumption is made that the velocity of the emitted particles, in the centre of mass system i.e. $\beta^x = \beta_c$. In fact there will be a distribution of the velocities of the emitted particles and consequently the above assumption is not strictly valid. Figure 4 shows the relation between the angle of emission in the centre of mass and laboratory systems for secondary particles whose velocities are given by $\beta_c/\beta^x = 0.95$, 1 and 1.2. It can be seen from this figure that only those particles emitted in the backward direction, in the centre of mass system, will be affected greatly by the assumption.

During the course of the present work an experiment has been completed (Goldsack et al. 1962) on the interactions of π^--mesons at 16.3 GeV in a hydrogen bubble chamber, in which the momentum distribution of the secondary π^--mesons and protons in the centre of mass system, has been determined. This has made it possible to estimate the affect of the momentum distribution on the Duller and Walker plot. Two angular distributions, in the centre of mass, have been used in calculating the Duller and Walker plot. One is an isotropic distribution and the other is one in which the intensity of the emitted particles varies as $\cos^2\theta$, θ being the angle of emission of the secondary particle in the centre of mass system. Figure 5

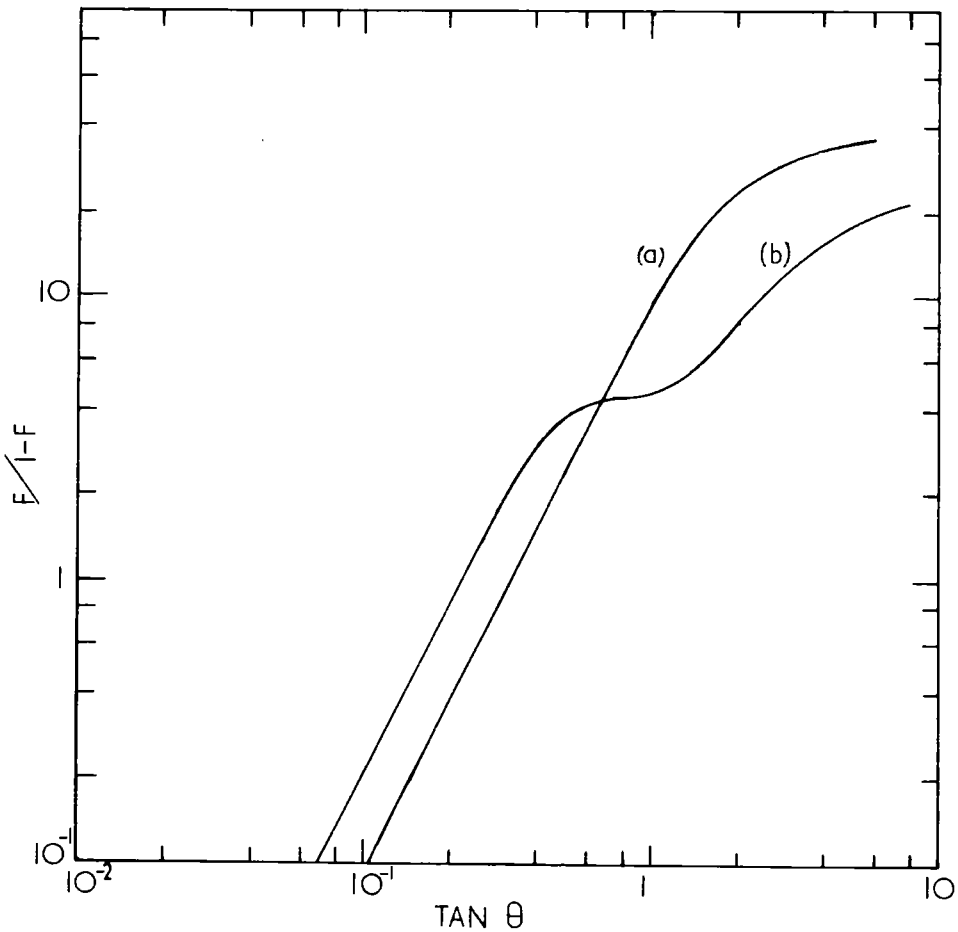

Fig. 5. The variation of $F/1-F$ with TAN θ for (a) an isotropic angular distribution in the centre of mass system and (b) a distribution given by $N(\varphi)\,d\varphi = \cos^2\varphi\,d\varphi$.

shows the variation of F/1-F with tan θ for these two distributions. From these curves it can be seen that the effect of the velocities of the secondary particles appears at larger angles i.e. about 50° - 60° in the laboratory system.

1.54 Conclusion

It can be seen from the preceding discussion that the analysis of nuclear interactions will be complicated by three factors, namely, the existence of secondary collisions, the continuing primary and the velocity distribution of the secondary particles. As seen above an allowance can be made for the velocity distribution. The correction for the effects of secondary collisions and the continuing primary will be discussed later.

CHAPTER 2

Preliminary Results on the Interactions of 16.3 GeV π^--mesons

2.1 Emulsion Stack and Exposure

A stack of 222 Ilford G.5 pellicles, each 29 cm x 14 cm x 600μ in size, has been exposed to the 16.3 GeV negative pion beam of the 25 GeV proton synchrotron at CERN Geneva. The beam is reported to have negligible electron contamination and about 10% contamination from muons. Of the stack 20 pellicles have been processed and scanned by this laboratory in order to carry out a study of the interaction of 16.3 GeV negative pions with complex nuclei.

Before exposure the stack is milled to provide each pellicle with two accurate reference edges. These reference edges enable the stack to be aligned very accurately with the beam. Accurate alignment ensures that the beam particles travel a large distance in each pellicle. After exposure the pellicles are located accurately with respect to a 'grid' which when illuminated produces a very shallow image on the bottom of each pellicle. Each square of the grid, which is 1 mm x 1 mm in size has two co-ordinates which give the position of the square with respect to the two reference edges. This arrangement facilitates the recording of the position of events and the following of tracks from one plate to another.

The processing of these plates is described in Appendix A1.

2.11 Scanning of the plates and the classification of the events

The plates have been scanned under a magnification of 45 x 1.5 x 15 on Cooke M4000 microscopes. Tracks are selected about 1 cm from the edge of the emulsion on which the beam is incident. The tracks are followed using the 'line scanning' technique until they are terminated by an interaction, by leaving the emulsion, or by merely reaching the end of the traverse of the microscope stage. The distance travelled along the track is noted and if an interaction occurs it is recorded and classified as a 'star' or a 'scattering'. An event is usually considered as a scattering if there is a perceptible change in the direction of the track at a particular point, whereas the sudden creation of any number of secondary particles at the termination ofthe track is called a star.

Initially the plate is set up so that the beam is parallel to one of the axes of the microscope. The eyepiece hairline is aligned parallel to the beam direction also. This facilitates the selection of beam tracks as opposed to the tracks of secondary particles. When a track is followed its direction is compared with the hairline every few fields of view. In this way it is possible to detect changes in direction of approximately $\frac{1}{4}^{o}$, using a reliable microscope stage.

When an event is recorded a detailed reference to the grid on the bottom of the emulsion is made in order that the event can be found again at some later date.

When a scattering is observed the scattered track is followed for a large distance. If the scattered particle giving rise to the track is an electron and not a π^--meson then it is usually scattered again after a few fields of view and can therefore be recognised and rejected. Both the secondary particles in events with two lightly ionizing particles are scrutinized in a similar way to eliminate events due to knock-on electrons.

When the scanning is complete all events are carefully checked a second time and co-ordinate measurements made on both the minimum and heavily ionizing secondaries in order that the angular distribution relative to the primary can be computed. The events are also classified according to the number of black, grey and minimum tracks n_b, n_g and n_s respectively. This classification is carried out visually. The grain densities of these groups of tracks are given by,

'black' tracks $6.8 < g^x$

'grey' tracks $1.4 < g^x < 6.8$

'minimum' tracks $g^x < 1.4$

where $g^x = \frac{g}{g_o}$, the normalised grain density. g_o is the grain density of tracks of plateau ionization.

The angular distribution of the minimum ionizing secondary particles is such that, generally, tracks are not long enough for measurements of their momenta to be made. In view of this the

analysis has consisted of a detailed study of the angular distribution of secondary particles.

Data from the events have been classified according to the number of minimum secondary particles n_s.

2.2 General Results

A total of 192.5 m of track has been followed in which there have been found 351 stars, 23 scatterings and 14 knock-on electrons. Since the knock-on electrons are produced without any appreciable change in the direction of the π^--meson they can be easily missed when scanning quickly. Consequently the high number of knock-on electrons observed is indicative of high scanning efficiency.

At 16.3 GeV the π^--mesons resulting from elastic diffraction scattering are highly collimated in the forward direction and the majority of the π^--mesons will be scattered at angles of less than 0.5°. However, the majority of scatterings have angles of scatter which are greater than 0.5° and have been classified as inelastic interactions in which all other secondary particles are neutral.

Events of the type $(1 + 0 + 1)$ and $(0 + 0 + 2)$ have been studied to select π^--p scatterings. Figure 6 shows the relation between the recoiling proton and the scattered π^--meson for an incident π^--meson energy of 16.3 GeV. Events of the type $(0 + 0 + 2)$ are plotted twice because it is not possible to distinguish between the π^--meson and proton. Events lying within the dotted lines will have recoiling protons with sufficiently high momenta to give rise

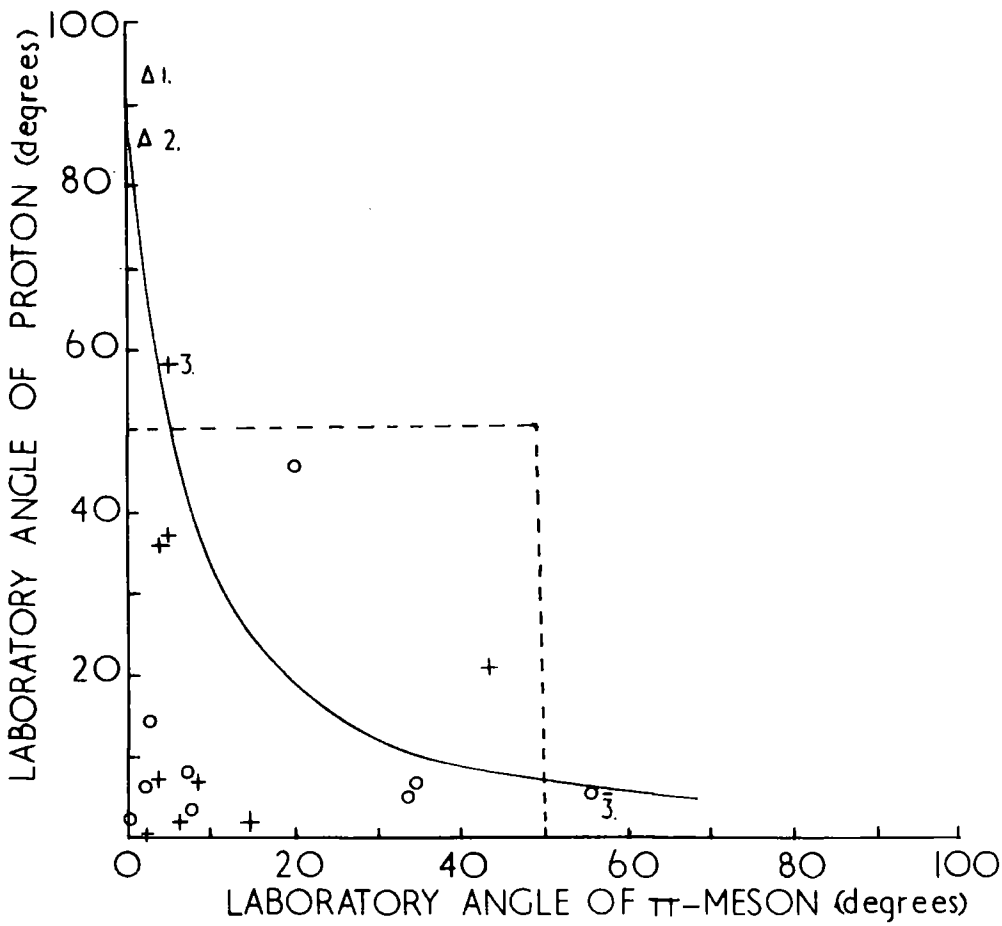

Fig. 6. The comparison of the observed and calculated angles of emission for possible $\pi^- - p$ elastic scatterings at 16·3 Gev.

to minimum tracks. Other events will have 'grey' or 'black' proton tracks emitted at large angles, and consequently are classified as (1 + 0 + 1) or (0 + 1 + 1) events. Events of this type are marked 1 and 2 in the figure, whereas event 3 is classified as (0 + 0 + 2). However, since it lies close to the accepted region for (0 + 0 + 2) events it is to be considered as a possible π^--p elastic scattering together with events 1 and 2. These three events must be subtracted from the total number of stars.

The corrected interaction length for π^--p elastic scattering is 57.75 metres giving a cross-section of 2.3 ± 1.1 mb. which compares with a value of 3.5 ± 0.5 mb. determined using a hydrogen bubble chamber (Goldsack 1962).

The total number of inelastic interactions is then 371 and taking the quoted contamination of 10% the mean free path for star production is 46.6 ± 2.4 cm. According to the optical model of Fernbach et al. (1949) this interaction length corresponds to an absorption coefficient of $K = (1.7 \pm 0.1) \times 10^{12}$ cm^{-1}. This can be compared with the expected value of $K = (2.4 \pm 0.2) \times 10^{12}$ cm^{-1}, calculated using the total cross-section for the interaction of π^--mesons with protons quoted by Goldsack (1962). This absorption coefficient corresponds to a mean free path in nuclear emulsion of (39.0 ± 1.5) cm. This discrepancy of (7.6 ± 2.9) cm. probably arises from uncertainty about the extent of the contamination of the beam.

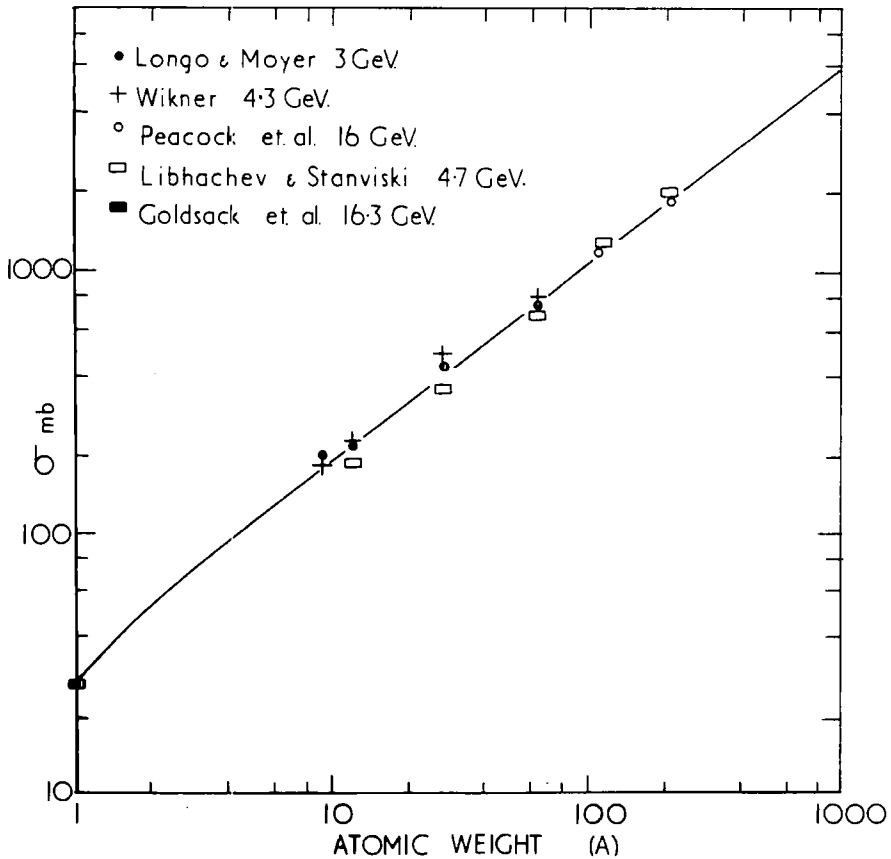

Fig.7. The variation of the total cross section with atomic weight for π−mesons.

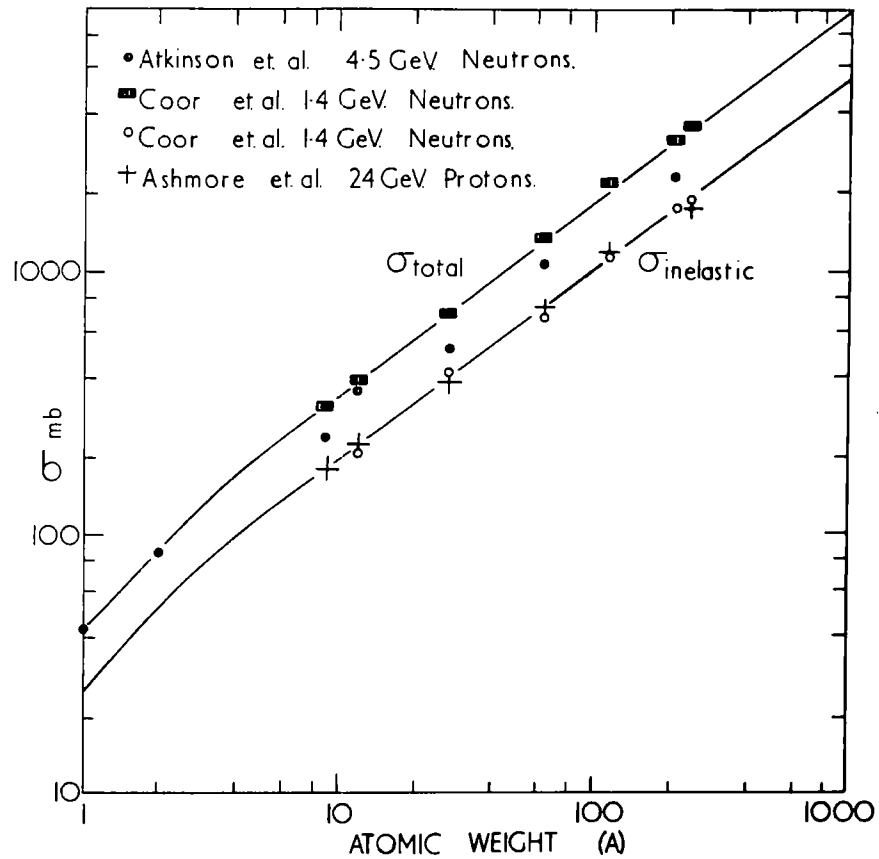

Fig.8. The variation of the total and inelastic cross sections with atomic weight for protons and neutrons

In figure 7 and 8 the available data has been collected together for the total cross-section for the interaction of π^--mesons and protons with the nuclei of beryllium, carbon, aluminium, copper, cadmium, tin, lead, bismuth, and uranium. For high energies the cross-sections appear to be independent of energy. From this data the mean free path for π^--meson interactions in nuclear emulsion has been calculated to be 37 cm. agreeing with the predicted value of the optical model. This implies a contamination of the beam of 21% which is well in excess of the quoted value of 10%. This conclusion has been verified by some detailed work on beam contamination carried out by the Milan group on plates from the same stack as the plates used in this laboratory. Although no absolute figure for the contamination has been determined, it has been established that the beam contamination is well in excess of the quoted 10%.

This conclusion invalidates the cross-section for the scattering of π^--mesons on hydrogen nuclei given earlier in this section. The corrected value of this cross-section, using the figure of 21% for the contamination, is 2.6 ± 1.5 mb.

Since the 23 scatterings have been classified as inelastic events it is not possible to make any further comparison with the optical model.

Figures 9, 10 and 11 show the distributions of the numbers of minimum, grey and black tracks. The average number of minimum

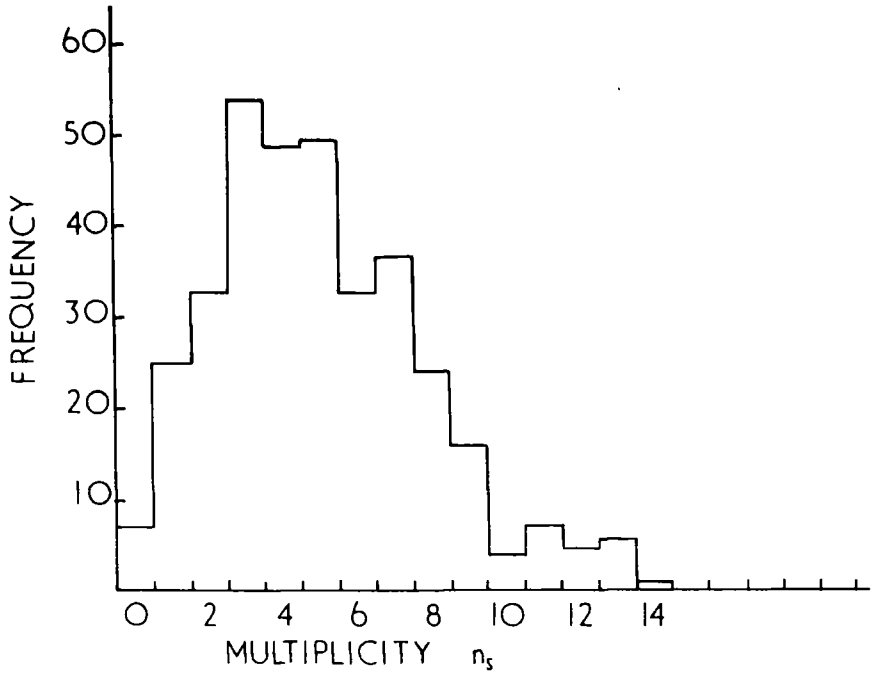

Fig.9. The distribution of minimum tracks for π^--nucleus interactions at 16·3 Gev.

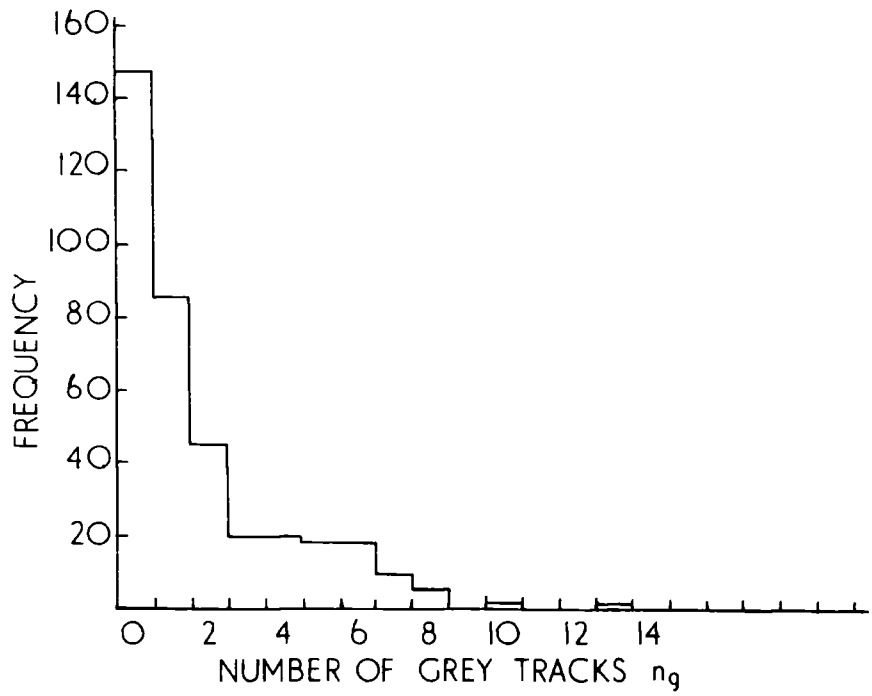

Fig.10. The distribution of grey tracks for π^--nucleus interactions at 16·3 Gev.

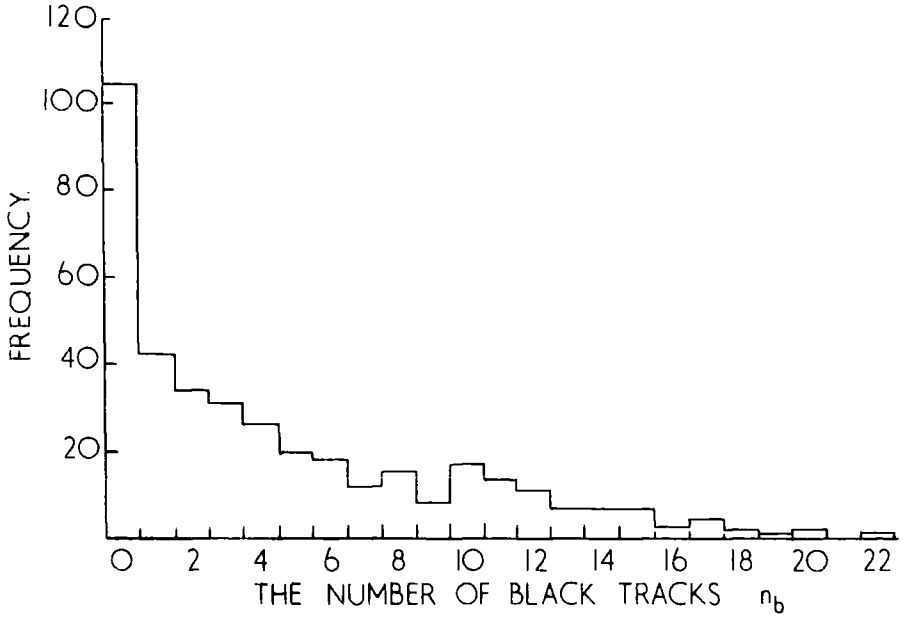

Fig.11. The distribution of black tracks for π^- – nucleus interactions at 16·3 Gev.

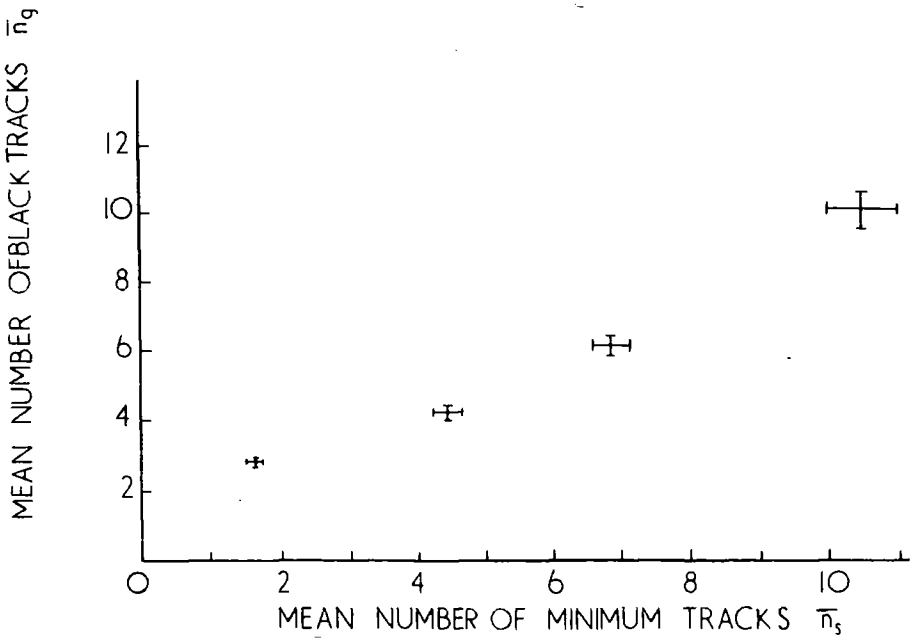

Fig.12. The relation between the number of black and minimum tracks for 16·3 Gev. π^- – nucleus interactions.

tracks is 4.77 ± 0.12 which compares with 3.82 ± 0.25 for the inelastic interactions of π^--mesons with protons (Goldsack 1962). The average number of heavy tracks is 6.40 ± 0.13 which is made up of 1.76 ± 0.07 grey tracks and 4.64 ± 0.11 black tracks. Further details of the distribution of events between the values of n_s, n_g and n_b, can be seen in Appendix A.2.

The difference in the average number of minimum tracks, between the π^--nucleus and π^--nucleon collisions is due to the existence of secondary collisions in the complex nuclei, giving rise to further π^--meson production. Further evidence for secondary collisions is shown by the increase of n_b with n_s, figure 12. The events with high excitation energy, usually attributed to several collisions, have large values of n_s.

2.3 Initial application of the Castagnoli and Duller and Walker Formulae

The interactions of 16.3 GeV π^--mesons with the emulsion nuclei have been analysed according to the methods of Friedlander. Of the 371 stars found by line scanning the spatial angles of all shower, grey, and black tracks for 310 stars have been measured. For each star a value of $\ell n\ \gamma_c$ using equation 8, has been computed. The distribution of $\ell n\ \gamma_c$ is shown in figure 13. The arrows indicate the expected value of $\ell n\ \gamma_c$ for π-π, π-2π, π-N and π-2N collisions at 16.3 GeV. The smooth curve indicates the normal distribution

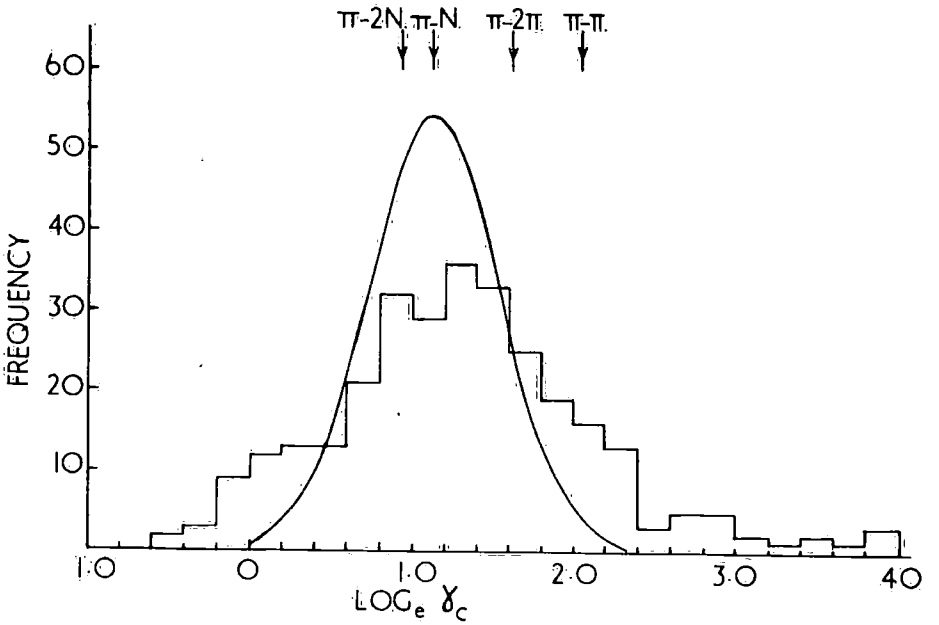

Fig. 13. The distribution of $\log_e \gamma_c$ for all events produced by 16·3 Gev. π^--mesons.

expected if only single π-N collisions occur. The deviation σ of the expected distribution is 0.41 and is given by $\sigma_o/\sqrt{n_s}$. σ_o is equal to 0.9 (Castagnoli 1953). The experimental distribution is much broader than the expected normal distribution. It can be seen from this distribution that there is no correlation between the experimental values and the expected values of $\ell n\ \gamma_c$ for π-π, π-2π, π-N and π-2N collisions. In fact the distribution is symmetrical about the value of $\ell n\ \gamma_c$ for the π-N collisions. At 16.3 GeV it is not possible to substantiate the observations of Friedlander (section 1.4).

Figure 14 shows how the value of $\ell n\ \gamma_c$ depends on n_s. The dotted line represents the expected value for $\ell n\ \gamma_c$ for a π-N collision. The very high values of $\ell n\ \gamma_c$ are typical of events with low n_s, whereas the very low values are typical of events with high n_s. Similar variations of $\ell n\ \gamma_c$ with n_s have been observed for the interactions, with complex nuclei, of 6.2 GeV protons (Winzeler et al. 1960), 9 GeV protons (Cuilli et al. 1962) and 27 GeV protons (Barbaro et al. 1961).

The Duller and Walker plots for the various values of n_s are shown in figures (i) and (xiv) of appendix A.3. Figure 15 shows one of these plots for $n_s = 4$. The solid line shows the expected variation of $F/_{1-F}$ with tan θ for an isotropic distribution of emitted particles, in the centre of mass system of a π-N collision.

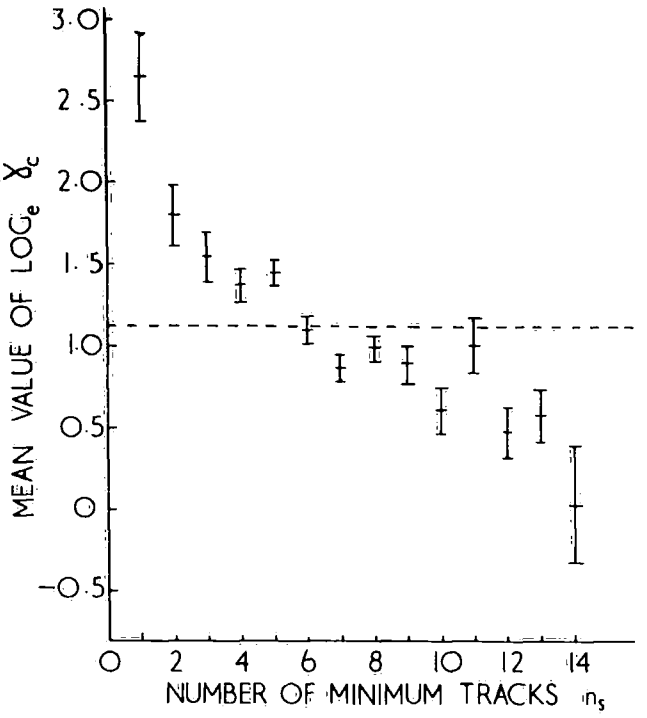

Fig.14. The relation between $\log_e \gamma_c$ and the number of minimum tracks for all events produced by 16·3 Gev $\pi^+\pi^-$ mesons.

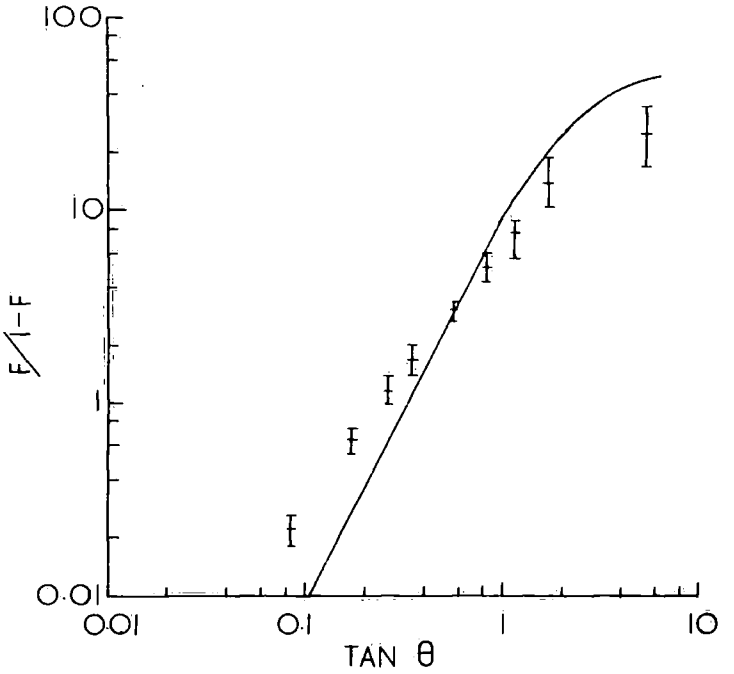

Fig.15. The Duller and Walker Plot for all tracks of the events with $n_s = 4$.

The position of the experimental points for each of the groups of n_s is systematically displaced to high values of tan θ as n_s increases. This corresponds to the decreases in $\ell n\ \gamma_c$ as n_s increases.

2.4 Deviations from the π-N Distribution

In section 1.5 the probable effects of secondary collisions, the continuing primary and momentum distribution of secondary particles in the centre of mass, have been discussed. The effect of the momentum distribution has been taken into account in the expected curve plotted on each of the figures A3(38) to (51v) and verifies the conclusion reached in section 1.5, i.e. that only particles emitted at very large angles in the centre of mass system will be affected greatly by the distribution of momentum.

Furthermore, it has been pointed out in section 1.5 that secondary collisions lead to a broadening of the angular distribution in the laboratory system, resulting in values of $\ell n\ \gamma c$ lower than expected. From figure 13 it can be seen that there are considerably more events with low values of $\ell n\ \gamma_c$ than expected and figure 14 shows that these events also have high values of n_s. This is consistent with the occurrence of secondary collisions.

In figure 13 it can also be seen that there are considerably more events with high values of $\ell n\ \gamma_c$ than expected. In figures A3(38) to (51) it can be seen that the slope of the straight portion

of the experimental curves is less than 2 for events with low n_s and tends to 2 as n_s increases. Moreover, figure 14 shows that the events with very high values of $\ell n\ \gamma_c$ are confined to those events with low n_s. These facts are consistent with the existence of the continuing primary which is more easily observed in events of low n_s.

It appears that the experimental evidence is consistent with the predictions of section 1.5.

The broad distribution of $\ell n\ \gamma_c$ is caused by the existence of secondary collisions and the continuing primary, which produced deviations from the expected distribution. The correlation with π-π, π-2π, π-N and π-2N collisions in the work of Friedlander is probably fortuitous.

Clearly before further analysis can be done events due to single collisions must be separated from those due to multiple collisions. This group must then have the continuing primary removed. A reasonable method for removing the continuing primary is to remove from the data of each star the track with the smallest angle of emission. In the majority of cases this track will, in fact, be the continuing primary.

The problem of selecting events due to single collisions will be discussed in the next section.

CHAPTER 3

Secondary Collisions

In this chapter the usual classification of interactions into those which have taken place in the light or heavy elements of the emulsion is not followed. Instead an attempt is made to classify the interactions according to the number of collisions which have taken place in the nucleus. This leads to a method of selecting nuclear interactions in which there has been only one collision.

The classification also leads to an estimate of the average cross-section for interaction of the secondary π-mesons with nucleons in the nucleus. This cross-section is consistent with the known value for π-mesons at 2.7 GeV which is the mean energy of the secondary particles. Furthermore a relation can be developed between the number of secondary collisions and the evaporation energy in the interaction.

3.1 The Initial Collision

It has been pointed out in section 1.52 that the probability for charge exchange for the interaction of π^--mesons with nucleons at 16.3 GeV is very small. Consequently a target proton or neutron will retain its identity after a collision. At 16.3 GeV it is highly probable that a target nucleon will acquire an energy greater than 1 GeV in a collision so that the recoiling target proton will

give rise to a track of minimum ionization in the emulsion. Such a target proton will be indistinguishable from the secondary π^--mesons which also give rise to minimum tracks.

In the work on π^--p interactions at 16.3 GeV (Goldsack 1962) it was possible to identify the target proton in 29% of the events. In these events the proton gave rise to a grey track.

In the case of collisions with neutrons, the target will not produce a track in the emulsion. The tracks observed in these events will be due to the continuing primary and the created particles and will be of minimum ionization.

If the assumption is made that there are equal numbers of collisions with protons and neutrons then only 14.5% of all interactions involving single collisions will have a grey secondary track.

In complex nuclei the initial collision is followed by secondary collisions of the primary and produced particles. In the average π^--p collision at 16.3 GeV 4 charged secondary particles are observed; one is the continuing primary, one the struck nucleon and two are the created π-mesons, which will be accompanied by one additional neutral π^o-meson. The total number of secondary particles is then 5 leading to an average energy for secondary particles of approximately 3 GeV. In their secondary collisions the target nucleon will not acquire a large energy. It is likely that these target protons will

leave grey tracks and consequently the number of grey tracks will give some information on secondary collisions. This conclusion is substantiated by the fact that for the interactions of 16.3 Gev π^--mesons with emulsion nuclei 61% of the events have one or more grey tracks whereas only 29% of the events in π^--p interactions are accompanied by a grey track.

This conclusion has also been reached by Zhdanov et al. (1960) who have shown that the integral angular distribution of grey tracks for the interactions of 8.7 GeV protons with emulsion nuclei is the same as the integral angular distribution of grey tracks for the interaction of 1.5 GeV π^--mesons with emulsion nuclei (Crew and Hill 1958). Figure 16 shows the integral angular distribution of grey tracks of Crew and Hill together with the experimental points from this laboratory for the interactions of 16.3 GeV π^--mesons with the nuclei of the emulsion. It can be seen that the agreement between the experimental points and the curve of Crew and Hill is very good. This is a strong indication that the grey protons result from collisions of particles with an energy close to 1.5 GeV. The average energy of the secondary particles produced by 8.7 GeV protons and 16.3 GeV π^--mesons is approximately 2 GeV and 3 GeV respectively which are similar to the 1.5 GeV of Crew and Hill. Consequently it can be concluded that the grey tracks result from collisions of the secondary particles.

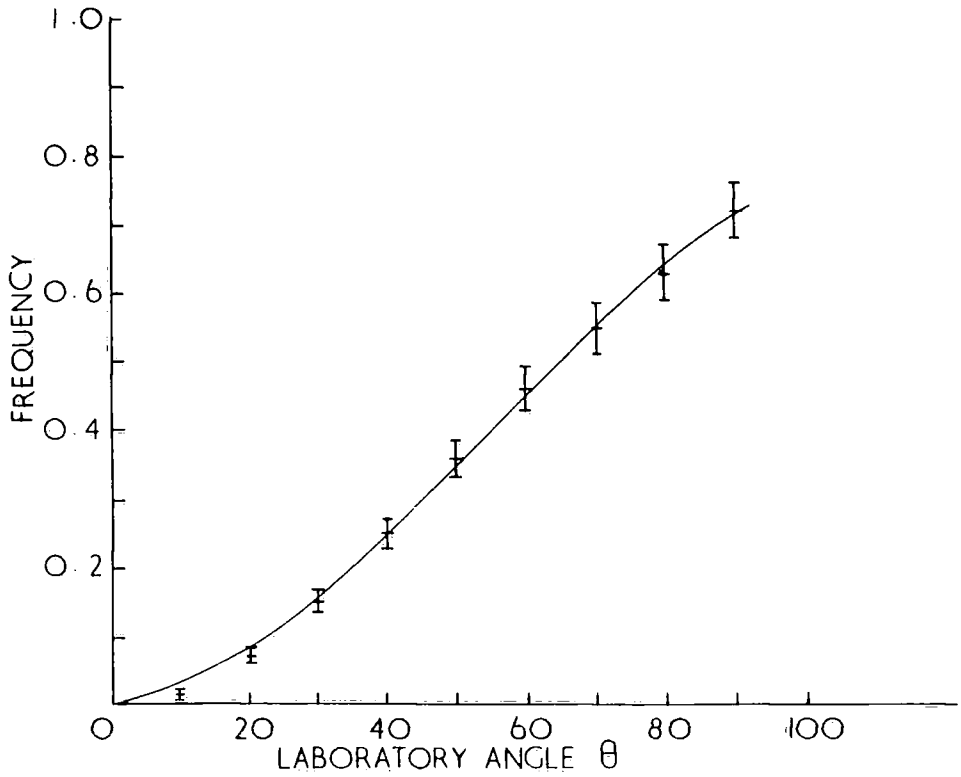

Fig.16. The integral angular distribution of grey tracks for 16·3 Gev. π^-–nucleus interactions. The full line is taken from Crew & Hill 1957 for the interaction of 1·5 Gev. π^--mesons with emulsion nuclei.

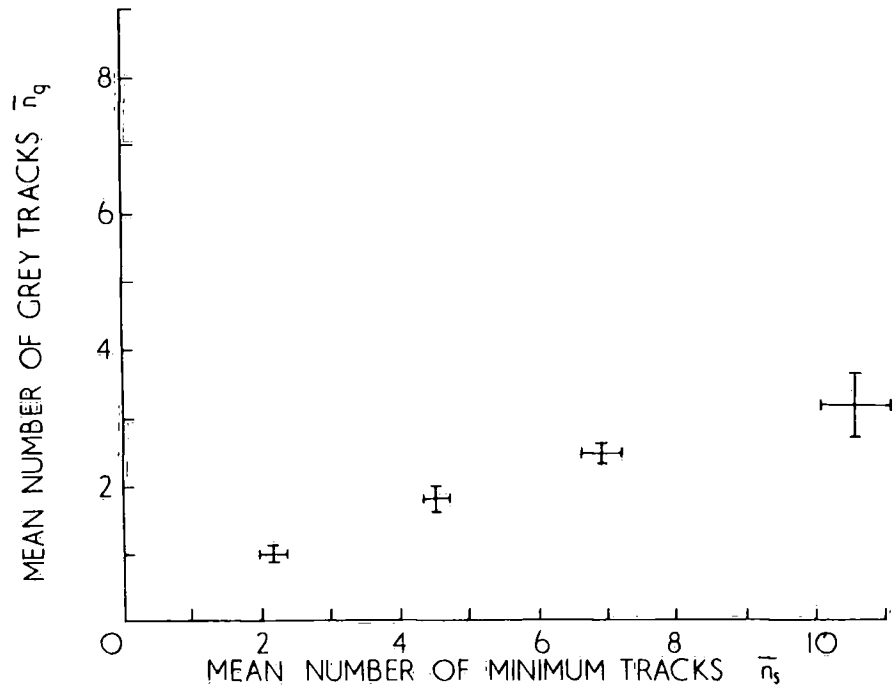

Fig.17. The relation between the numbers of grey and minimum tracks for 16·3 Gev. π^--nucleus interactions.

This discussion leads to the conclusion that the group of events with $n_g = o$ will consist predominantly of events in which there are no secondary collisions. The group of events with $n_g = 1$ will on average correspond to interactions in which there has been the initial collision and two secondary collisions i.e. one collision with a proton and one with a neutron. It follows that the total number of collisions n_c, will be given by the equation $n_c = 2n_g + 1$. This equation will only be an approximate relation but it is expected to apply for low values of n_g and to become less exact at high values.

3.11 The Relation between the Number of Grey Tracks and the Number of Minimum Tracks

From the preceding section it has been concluded that the number of grey tracks indicates the number of secondary collisions. It follows then that as n_s increases the probability of secondary collisions increases and consequently the average value of the number of grey tracks should also increase.

Figure 17 shows the relation between $\bar{n}_g$ and $\bar{n}_s$ and it can be seen that $\bar{n}_g$ increases steadily with $\bar{n}_s$.

An estimate of the average cross-section for interaction of the secondary particles on a single nucleon can be obtained from the average number of grey tracks together with the average number of minimum tracks produced in a single nucleon collision.

From the average value of $\bar{n}_g = 1.76 \pm 0.07$ it is estimated from above that 3.52 ± 0.10 secondary collisions occur on average. The average number of fast particles after the initial collision is 4.07 ± 0.12 leading to an average probability for interaction of $86 \pm 3.5\%$. The average potential path length of secondary particles has been calculated, for the interaction of 16.3 GeV π^--mesons with emulsion nuclei, in appendix A.4 and is 3 fermis leading to the mean free path in nuclear matter corresponds to an average cross-section of (29.4 ± 1.2) mb.

If on average, the secondary particles consist of the continuing primary, target nucleon, 2 created charged π-mesons and 1 neutral π-meson which have cross-sections for interaction with nucleons of 30, 43, 30 and 10 mb respectively, the expected average cross-section is 29 mb. This is in reasonable agreement with the estimate based on the average number of grey tracks. This confirms the method of estimating the number of secondary collisions from the number of grey tracks.

3.12 The relation between the Multiplicity and the Number of Grey Tracks

Using the expression $n_c = 2n_g + 1$ to give the total number of collisions and assuming that the charged particle multiplicity for secondary collisions is that given by Figure 3 for interactions of

π-mesons of 3 GeV with free nucleons, a variation of the mean value of n_s for the groups of events with $n_g = 0$, 1, 2 and 3 has been calculated.

The straight line of figure 18 shows the expected relation between $\bar{n}_g$ and $\bar{n}_s$. The agreement between the experimental point and this line is good between $\bar{n}_g = 0$ and 3.5. Between $n_g = 3$ and 6 the value of $\bar{n}_s$ does not appear to change and this is probably due to the saturation in the number of collisions that take place. The events of $\bar{n}_g = 3.5$ will probably have a greater proportion of secondary target protons than the usual 50%.

3.13 The Relation between the Number of Grey Tracks and the Number of Evaporation Tracks

In section 2.2 the variation of n_b with n_s indicated an increase of excitation energy with increase of n_s. This has been attributed to the effects of secondary collisions. Since the number of grey tracks varies with n_s in a similar way it is expected that n_b will increase with n_g. This variation is shown in Figure 19 and the expected increase of n_b with n_g is clearly visible.

Until now it has not been possible to derive a quantitative relation for the variation of evaporation energy, which is characterised by n_b, and the number of grey tracks. However, some recent work by Gooding and Pugh (1960) and Pugh and Riley (1961) indicates that it is possible to predict the relation between the evaporation energy and the number of nucleons removed from the nucleus.

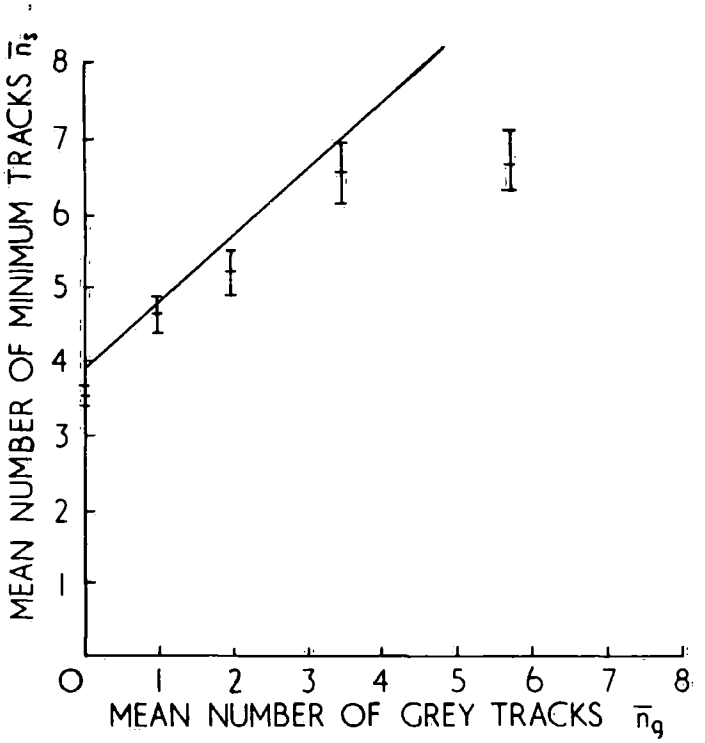

Fig.18. The relation between the average numbers of minimum and grey tracks for 16·3 Gev. π^-–nucleus interactions.

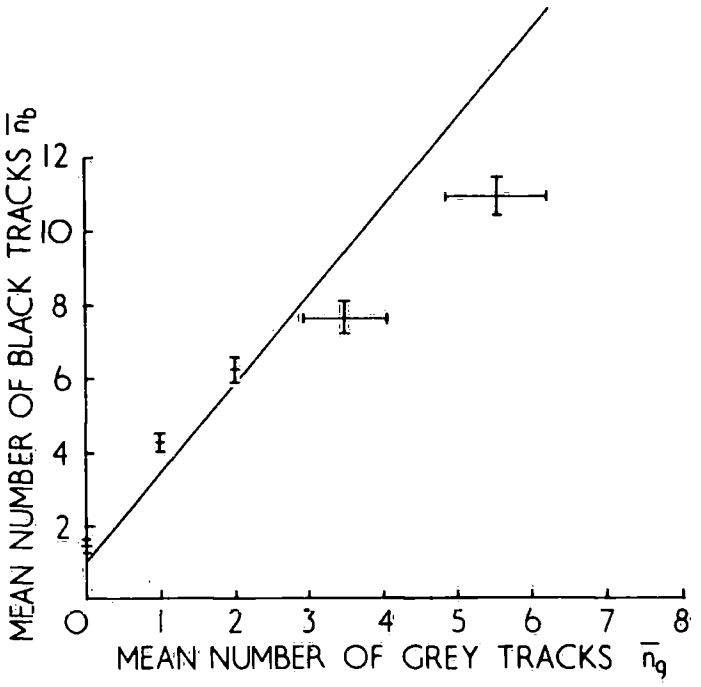

Fig.19. The relation between the number of evaporation tracks n and the number of grey tracks for 16·3Gev. π^--nucleus interactions.

Gooding and Pugh and Pugh and Riley have examined the (p,2p) reaction at 140 MeV. They have found that the sum of the energies of the secondary protons is smaller by 40 MeV than the energy of the primary proton, when a proton is removed from a nucleus of Z = 20. This energy difference leads to the excitation of the nucleus when a single nucleon is removed. In the following discussion it will be assumed that the value of 40 MeV also represents the excitation energy for each nucleon that is removedfor all nuclei.

It is then possible, on these assumptions, to determine the number of evaporation tracks emitted from a nucleus. The interaction between an incident particle and a nucleus can be expressed energetically by:-

$$W_1 + W(A,Z) = W_2 + W_g + W[(A-n), (Z-p)] + n'W' + (p - 2n' - n_{gp})W_p + (n - 2n' - n_{gn})W_n \quad \ldots\ldots 13$$

where W_1 is the total energy of the bombarding particle, W(A,Z) the total energy of the struck nucleus, W_2 is the total energy of the primary particle after the interaction together with the total energy of the created particles. n_{gp} and n_{gn} represent the number of grey protons and neutrons removed from the nucleus. These target particles have a total energy of W_g. p and N are the numbers of

evaporation protons and neutrons which have average total energies of W_p and W_n respectively. n' is the number of alpha particles emitted with an average total energy of W'. W[(A-n),(Z-p)] is the total energy of the final nucleus.

The equation 13 can be written in the form

$$W_1 - W_2 - E_g = \boxed{W[(A-n)(Z-p)] + n_{gp} M_p + n_{gn} M_n + n' M' + (p - 2n' - n_{gp})M_p + (n-2n' - n_{gn})M_n - W(A,Z)} + n'E' + (p-2n' - n_{gp}) \bar{E}_p + (n-2n' - n_{gn}) \bar{E}_n \quad \ldots\ldots 14$$

The terms in equation 14, enclosed by the dotted line represent the binding energy of the various groups of nucleons. Substituting now the number of black tracks observed in an event n_b, and F as the fraction of black tracks which are due to α particles then equation 14 can be written

$$W_1-W_2-E_g = (1-F)n_b \ (\overline{BE} + \bar{E}_p) + 1.2(1-F)n_b \ (\overline{BE} + \bar{E}_n) + Fn_b(\overline{BE}'+\bar{E}') \quad \ldots\ldots 15$$

The quantity F has been determined experimentally by Lees et al. (1953) and is given for various values of n_b. $\bar{E}_p + \bar{E}'$ have been taken from the data of Le Couteur (1950) and $\bar{E}_n$ from Skyrme (1962). It has also been assumed that on average the ratio of evaporation neutrons to evaporation protons is 1.2 : 1.

$W_1-W_2-E_g$ represents the energy which is lost to the nucleus during an interaction. This will be 40 MeV for the primary collision

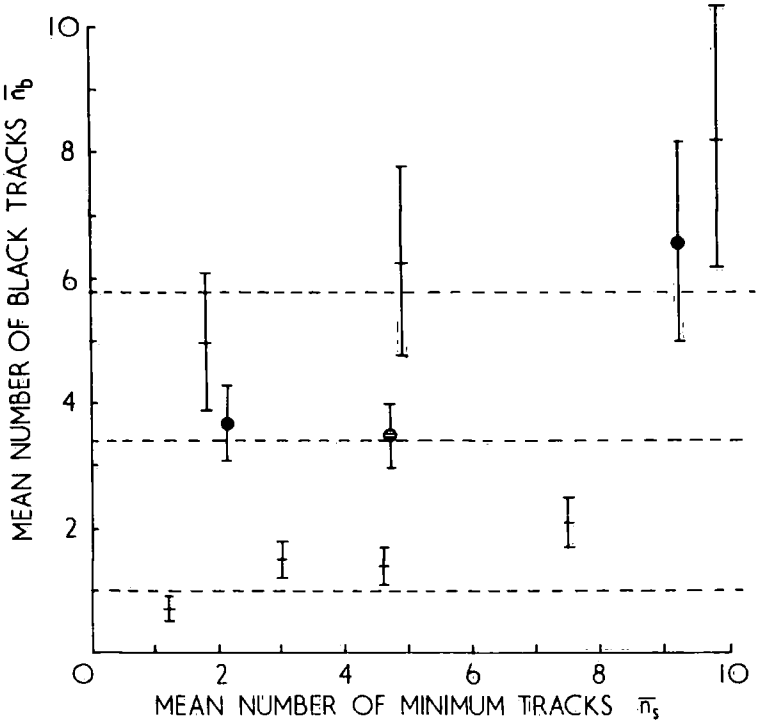

Fig. 20. - The relation between the number of evaporation tracks and the number of minimum tracks for events produced by 16·3Gev. π^--mesons.

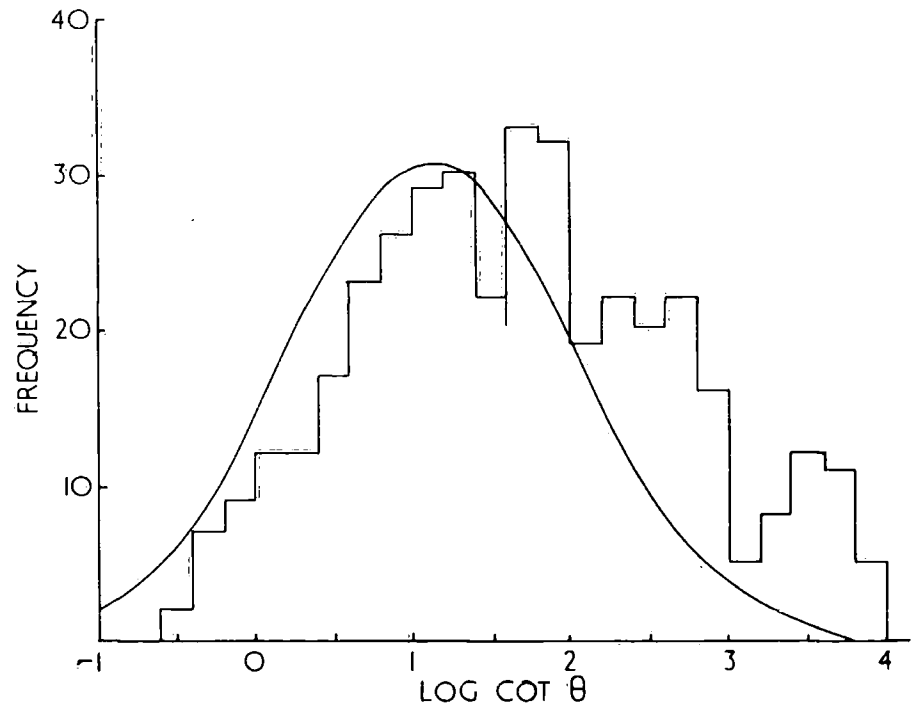

Fig. 21. The distribution of $\log_e \cot\theta$ for all tracks of events produced by 16·3 Gev. π^--mesons with $n_g = 0$.

and 40 MeV for each secondary interaction. The average number of black tracks as a function of the total number of collisions can now be determined. The results of this simple calculation are shown as the straight line in Fig. 19. The agreement between the expected line and the experimental points is not good but there is sufficient agreement to conclude that the calculation is correct in general concept if not in detail.

From the preceding discussion it can be seen that the number of collisions is given by $n_c = 2n_g + 1$, this expression being more significant for the lower values of n_g. It follows from this approach that a group of events with constant n_g should have a constant average number of evaporation tracks for the various values of n_s. In fact for $n_g = o$ the average n_b is expected to be 1.0 from Figure 19 and for $n_g = 1$ and 2, $\overline{n}_b$ is expected to be 3.4 and 5.8 respectively.

Figure 20 shows the variation of $\overline{n}_b$ with n_s for groups of events with constant n_g of 0, 1 and 2, together with the expected values of $\overline{n}_b$. Again the agreement is only sufficient to indicate that the general approach is correct and that the calculation must be refined to explain the various deviations.

3.14 Conclusion

In sections 3.10 - 3.13 it has been shown that the number of grey tracks gives a good indication of the number of secondary collisions taking place in a nucleus, particularly for low values

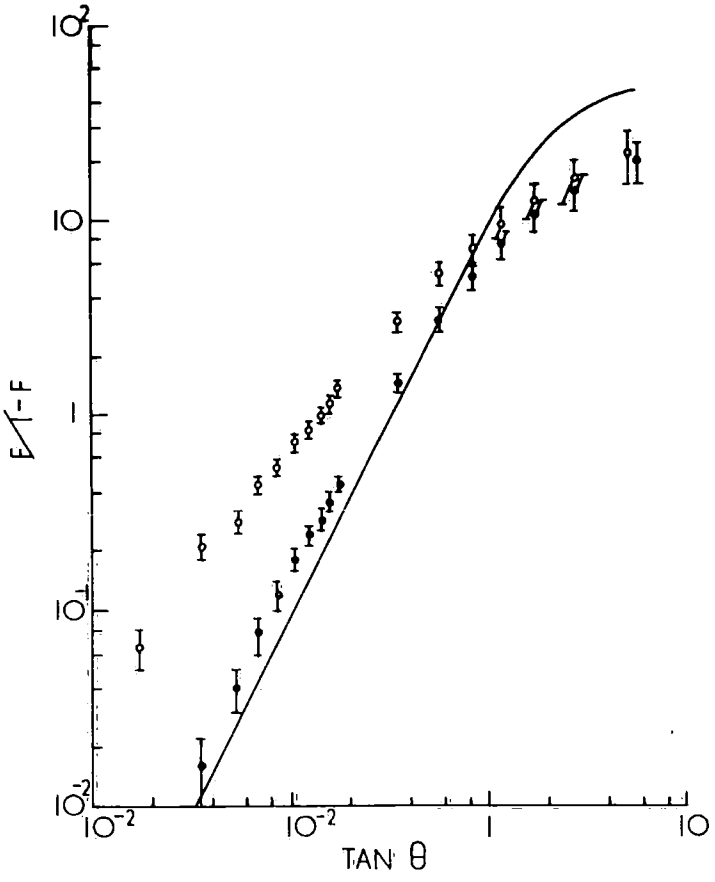

Fig.22. The Duller & Walker Plot for events produced by 16.3Gev. π^--mesons with $n_g=0$; (a)•, all tracks and (b)•, excluding the continuing primary.

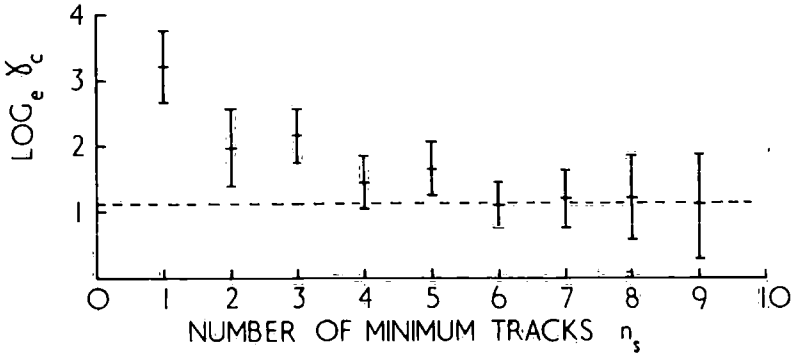

Fig.23. The relation between $\log_e \gamma_c$ and the number of minimum tracks for events produced by 16.3Gev. π^--mesons with $n_g=0$.

of n_g. The principal conclusion here is that the group of events with $n_g = o$ is dominated by events in which there are no secondary collisions.

3.2 Analysis of Single Collision Events

From the preceding section it is evident that the group of events with $n_g = o$ is dominated by single π-meson - nucleon interactions. This group of events has now been analysed similarly to the analysis of section 2.3.

Figure 21 shows the distribution of $\ell n \cot \theta$ for all the tracks of the group of events with $n_g = o$. The smooth curve represents the expected distribution of these tracks. Figure 21 should be compared with figure 13 which is for all values of n_g. From figure 21 it can be seen that there is a considerable excess of tracks with high values of $\ell n \cot \theta$. This excess is also seen in the Duller and Walker Plot, (figure 22).

Figure 23 shows the variation of $\ell n \gamma_c$ with the number of minimum tracks, n_g. It can be seen that for events with $n_s = 1$, 2, 3, 4, and 5 the value of $\ell n \gamma_c$ is slightly higher than expected while for events with $n_s = 6$, 7, 8 and 9 the agreement with the expected value of $\ell n \gamma_c$ is very good. This is consistent with the effect of the continuing primary discussed in section 1.5. Since charge exchange is a very unlikely process (Menon, private communication) then the value of $\ell n \gamma_c$ for those events with $n_s = 1$ must be typical of the continuing primary.

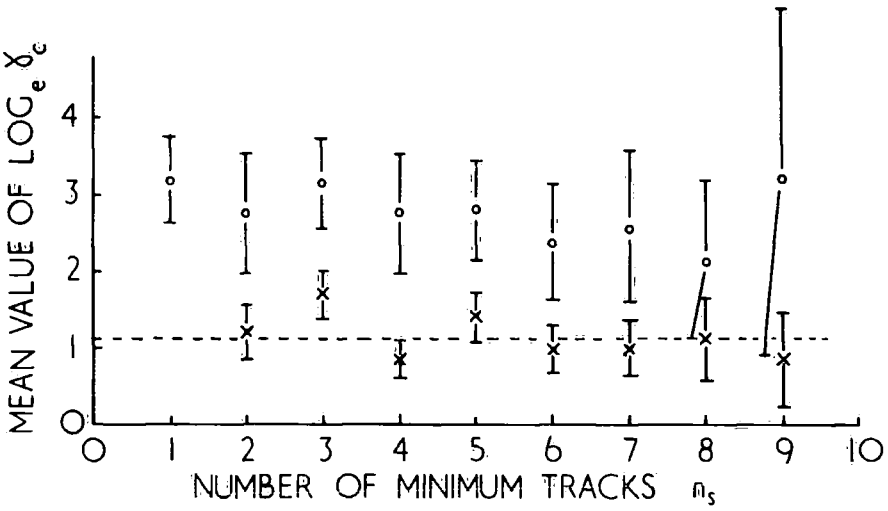

Fig. 24. The relation between the corrected value of $\log_e \gamma_c$ and the number of minimum tracks for events produced by 16·3Gev. π^--mesons with $n_g=0$.
∘ ln cot θ for the discarded particle.
× corrected $\log_e \gamma_c$

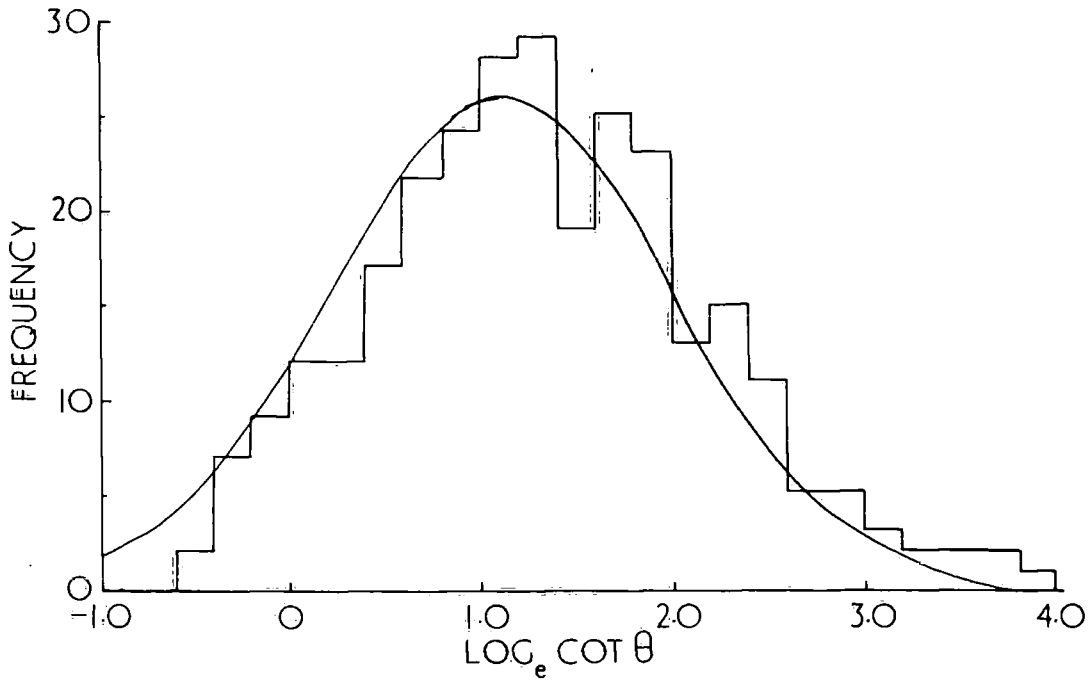

Fig. 25. The distribution of $\log_e \cot\theta$ for events produced by 16·3Gev. π^--mesons with $n_g=0$ and excluding the continuing primary.

The track with the smallest angle of emission has been eliminated from each event, and a new value of $\ell n\ \gamma_c$ has been calculated. The values of $\ell n\ \gamma_c$ calculated in this way are shown in figure 24, together with the mean value of ℓn cot θ for the discarded particle assumed to be the continuing primary for each group of constant n_s. The agreement with the expected value of $\ell n\ \gamma_c$ is now good. Thus the Castagnoli formula leads to the correct result for single collisions when a correction for the continuing primary is made. The average values of ℓn cot θ for the discarded particles are constant with the value of ℓn cot θ for events with $n_s = 1$. which justifies the assumption that these particles are the continuing primary.

Figures 22 and 25 show the distribution of ℓn cot θ and Duller and Walker plot, after removing the continuing primary particles, together with the expected distributions. From these figures it can be seen that there is still a slight excess of high values of ℓn cot θ.

It has been suggested by Zhdanov (private communication) that events with $n_g = 1$ are also single collision events. From the work of Goldsack et al. (1962) the number of single collision events with $n_g = 1$ expected in the present work is 27. However, 86 events with $n_g = 1$ have been observed. Figures 26, 27 and 28 show the distribution of ℓn cot θ and the Duller and Walker plot for these events, and figures it can be seen that the experimental points are in good agreement with the expected curves.

Figure 29 shows the Duller and Walker plot both with and without the continuing primary, for interactions with $n_g = o$ and 1 produced

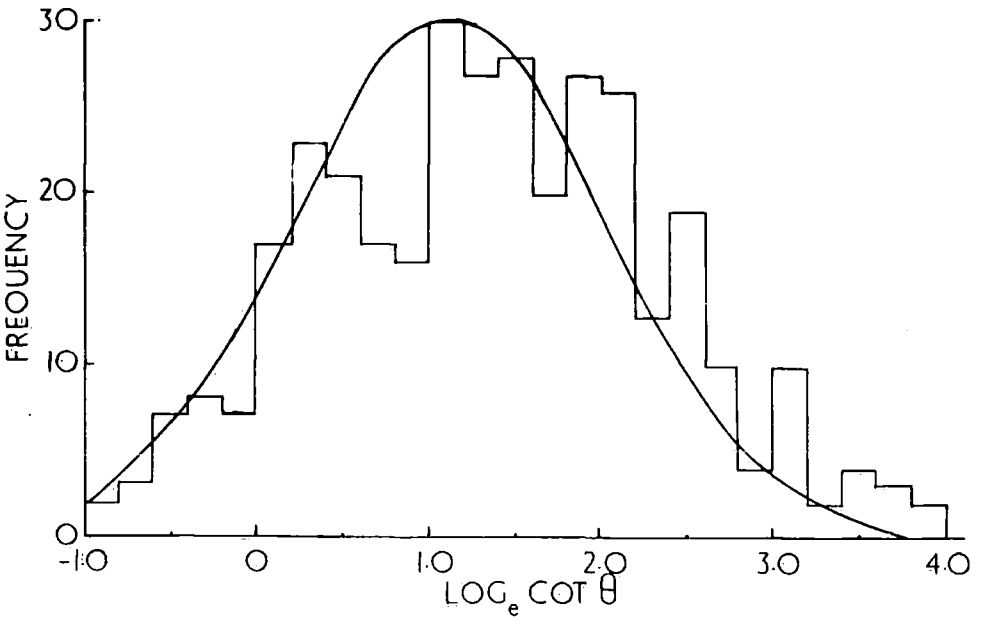

Fig. 26. The distribution of $\log_e \cot\theta$ for all tracks of events produced by 16·3 Gev. π^--mesons with $n_g = 1$.

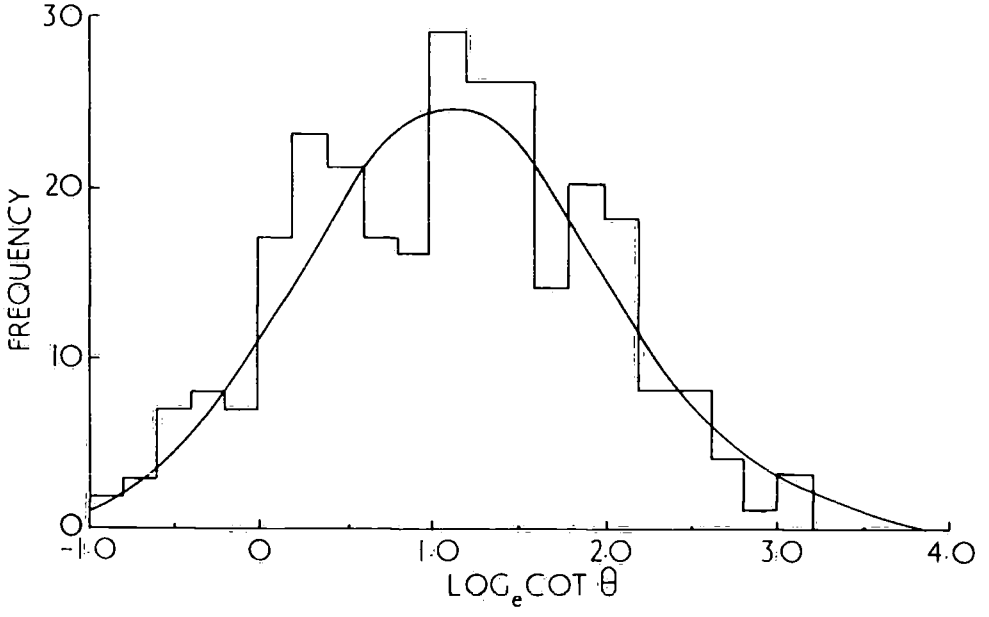

Fig. 27. The distribution of $\log_e \cot\theta$ for events produced by 16·3 Gev. π^--mesons with $n_g = 1$ and excluding the continuing primary.

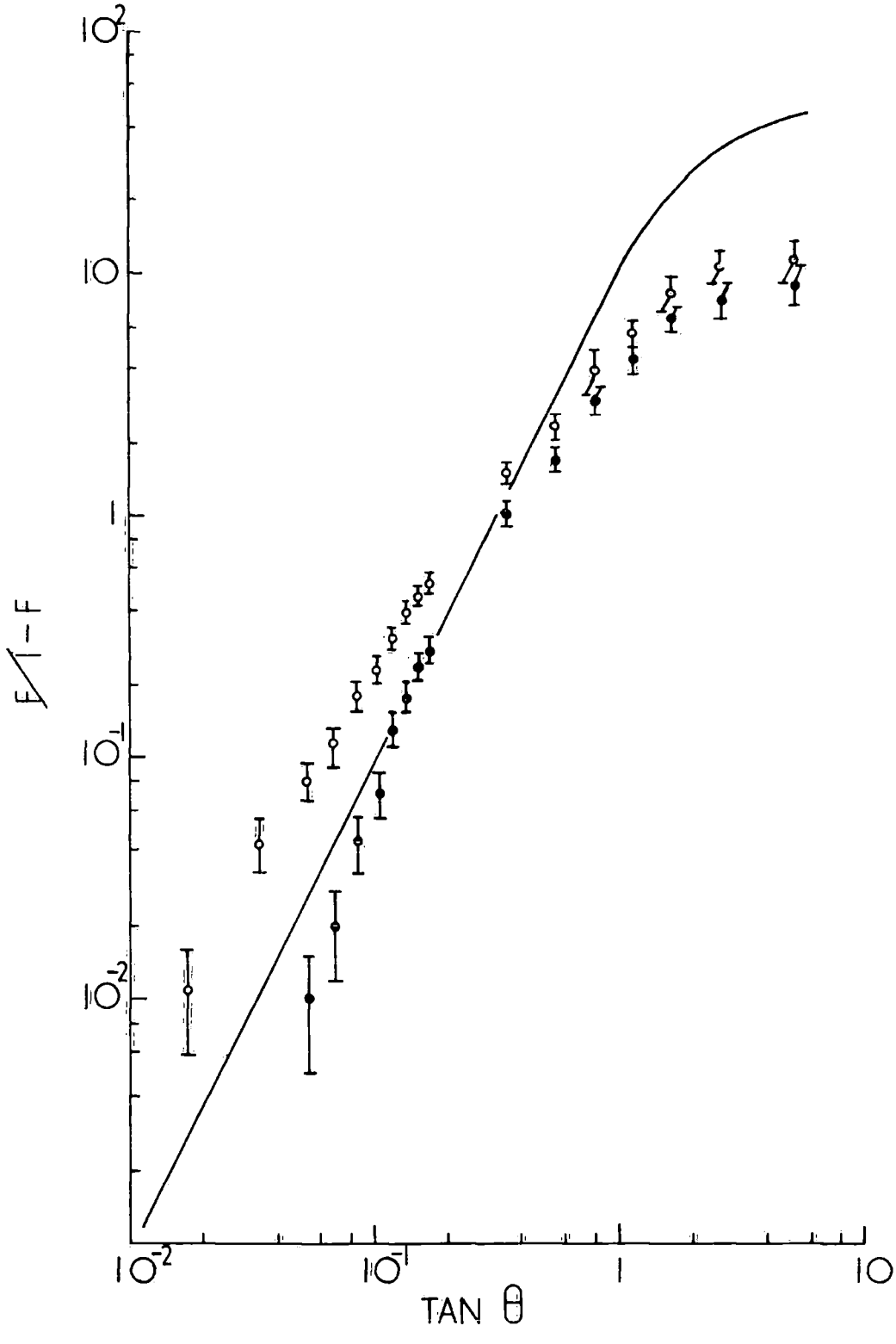

Fig. 28. The Duller & Walker Plot for events produced by 16·3Gev. π^--mesons with $n_g = 1$; (a) ∘, all tracks and (b) •, excluding the continuing primary

by 25 GeV protons in emulsion. Again it can be seen that the agreement between the corrected curve and the expected curve is very good, giving further weight to this method of selecting single collision events. (Williams, Thesis 1962)

3.3 Differences between events with high and low values of n_s

It has been mentioned in the previous section that, even after correcting for the continuing primary, there is still a slight excess of high values of $\ell n \cot \theta$. If only one collision takes place then only collisions with targets lighter than one nucleon can lead to values of $\ell n \cot \theta$ higher than the expected values. It is therefore, of interest to see if the results are in agreement with the assumption that a proportion of the events are due to collisions with a π-meson in the meson cloud of the nucleon.

The events with $n_g = o$ have been divided into two groups, those events with $n_s = 2, 3, 4$ and 5 and those with $n_s > 5$. Figures 30 and 31 show the distribution of $\ell n \cot \theta$ and the Duller and Walker plot for events with $n_s > 5$. In each case an expected curve is drawn for comparison. For these events the experimental results are in agreement with the created particles being emitted isotropically in the centre of mass system.

Figures 32 and 33 show the same distribution for events with $n_s \leqslant 5$. In this case there is poor agreement between the experimental results and the expected curve, (a), for an isotropic angular distribution of particles in the centre of mass system. However, these distributions are in agreement with an equal number of tracks emitted

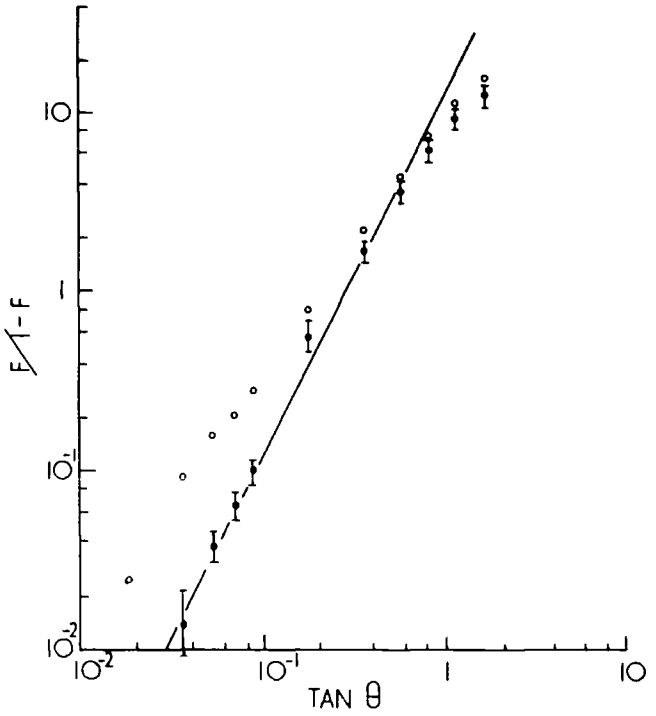

Fig. 29. The Duller & Walker Plot for events produced by 25Gev. protons with $n_g = 0$ and 1; (a) ∘, all tracks and (b) •, excluding the continuing primary.

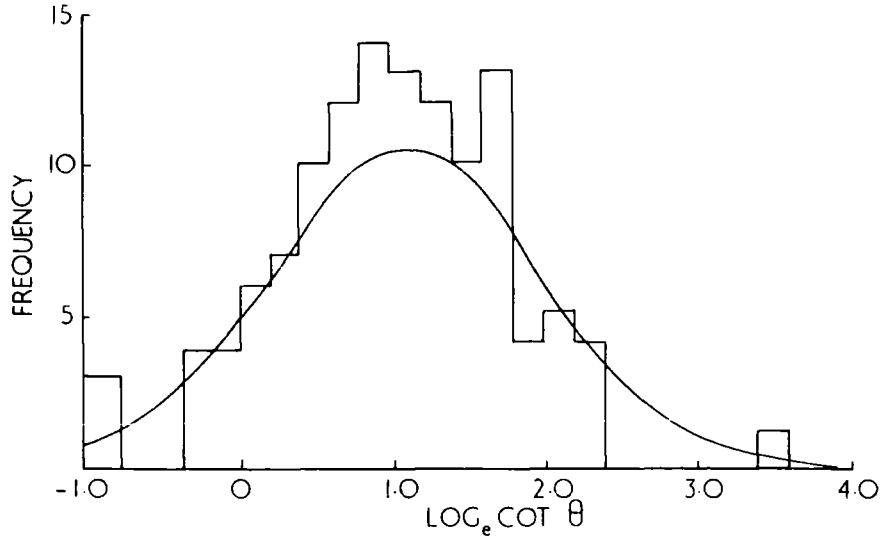

Fig. 30. The distribution of $\log_e \cot\theta$ for events produced by 16·3Gev. π^--mesons with $n_g = 0$, $n_s = 6, 7, 8, \& 9$, excluding the continuing primary.

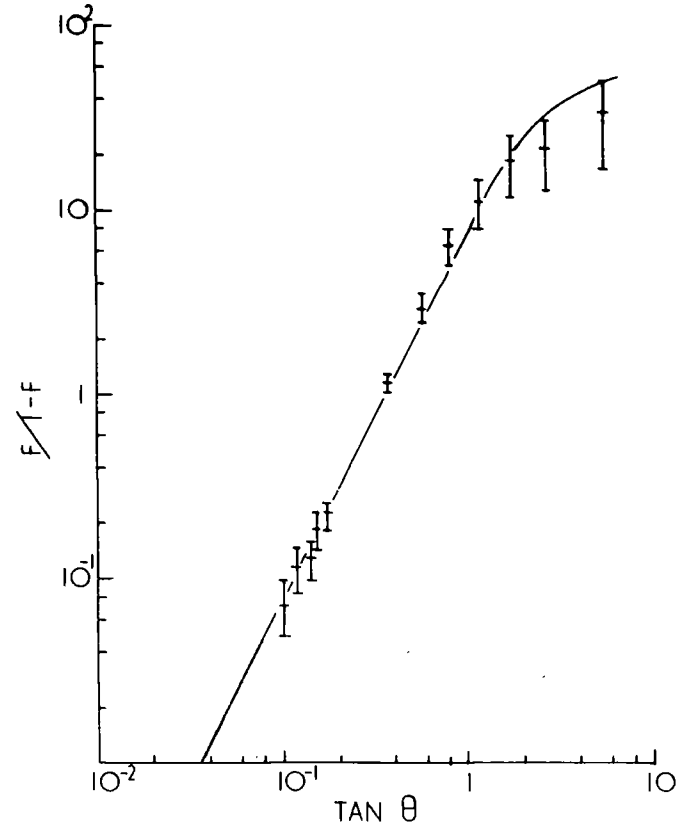

Fig.31. The Duller & Walker Plot for events produced by 16·3 Gev. π^--mesons with n_g=O, n_s=6,7,8 & 9, excluding the continuing primary.

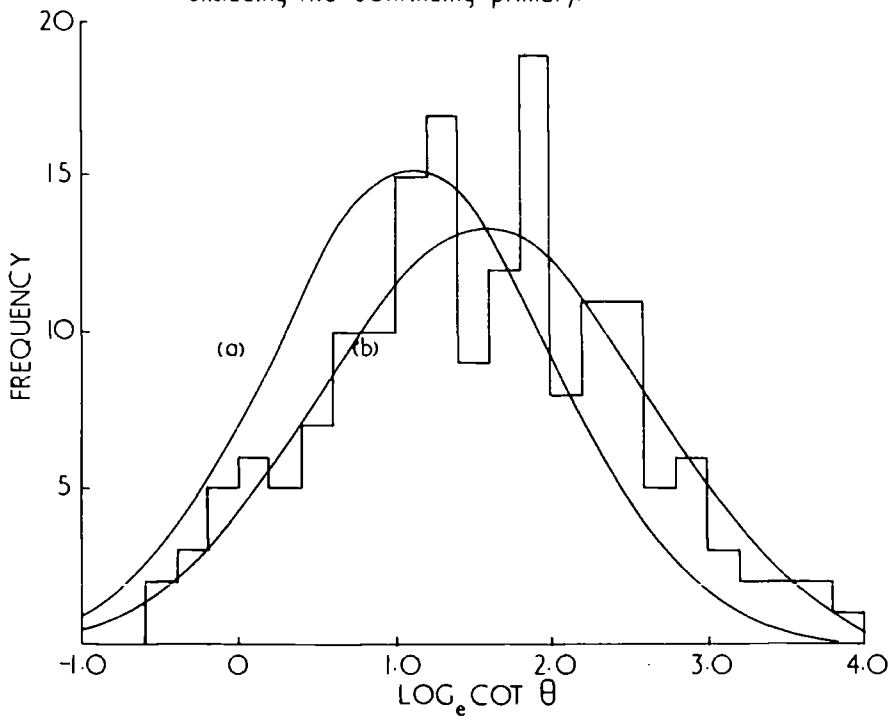

Fig.32. The distribution of $\log_e \cot \theta$ for events produced by 16·3 Gev. π^--mesons with n_g=O, n_s= 2,3,4 & 5, excluding the continuing primary.

isotropically in the centre of mass systems for π-meson-nucleon and π-meson - π-meson collisions, curve (b).

Figure 34 shows the distribution of $\ell n\ \gamma_c$ for these events and for comparison an expected curve is drawn based on the assumptions that half the events are due to collisions between the incident π-meson and a π-meson in the meson cloud of the nucleon, and half are due to collision between the incident π-meson and a nucleon and that the width of each distribution is given by $\sigma_{\ell n \gamma_c} / \sqrt{\pi_s} = 0.48$.

There is general agreement between the expected curve and the histogram. On the basis of the measured events and correcting for those single collision events with $n_g = 1$, 32% are consistent with a collision between the incident π-meson and a π-meson in the cloud of a nucleon. This compares with a value of 30% determined by Bozoki et al. (1962) in a study of π^--meson-nucleon interactions at 7.3 GeV.

3.4 Conclusions

In the preceding sections it has been shown that the group of events with $n_g = o$ consists predominantly of single collision events. However, figures 27 and 28 show that the angular distribution of minimum tracks for events with $n_g = o$ and 1 are in agreement with the expected distributions of Castagnoli and Duller and Walker, showing that in general the secondary particles (other than the incident π-meson) are produced isotropically in the centre of mass system for a collision between the incident π-meson and a stationary nucleon.

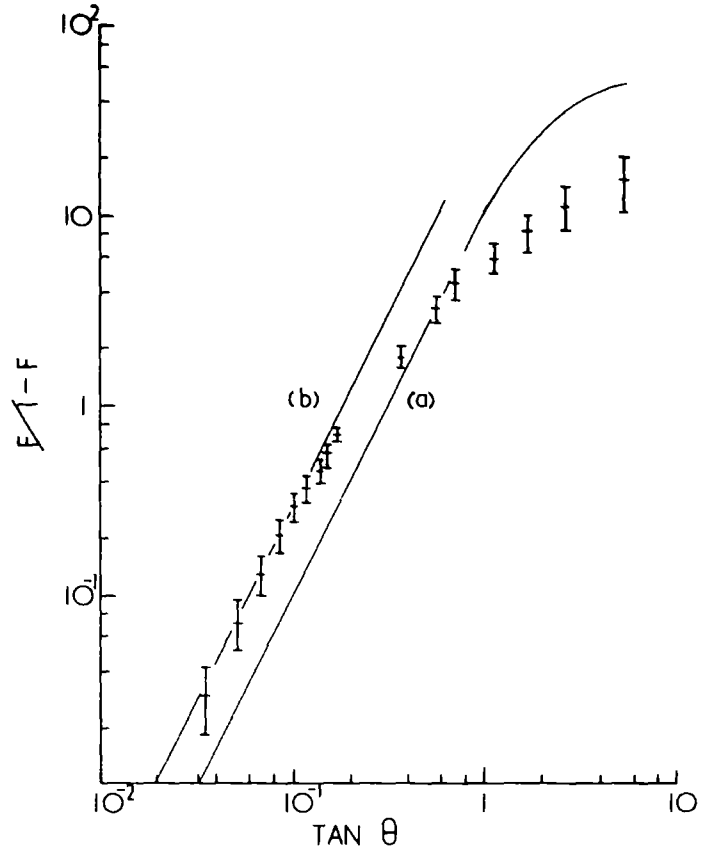

Fig.33. The Duller & Walker Plot for events produced by 16·3 Gev. π^--mesons with $n_q = 0$, $n_s = 2,3,4$ & 5 excluding the conuing primary.

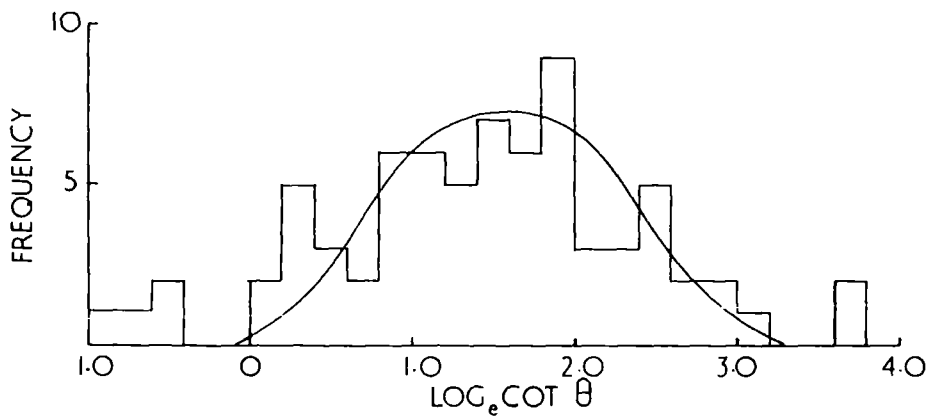

Fig.34. The distribution of $\log_e \gamma_c$ for events produced by 16·3Gev. π^--mesons with $n_q = 0$, $n_s = 2,3,4$ & 5 excluding the continuing primary.

The events with $n_g = 1$ have a somewhat higher excitation energy than is expected for events due to only one collision. Consequently the selection of events with $n_g = 0$ and 1 will lead to a sample of events which are contaminated by events in which more than one collision has occurred.

Selection of events with $n_g = o$, however, will give a sample of events with considerably less contamination from multiple collision events but in this case some genuine single collision events with $n_g = 1$ will be overlooked.

In the past, single collision events have been selected by taking those with $n_h < 5$ and this method of selection restricts the range of values of n_s which are attributed to single collisions. A more restrictive selection has also been used where events with 0, 1 and 2 heavy prongs are selected. However, the selection events with $n_g = o$ gives a good sample of single collision events even though n_b ranges from 0 to 9.

For those events in which more than one collision occurs it is found that the properties of the interaction can be understood in terms of a cascade process in which the nucleons appear to act independently. A consequence of the fact that the nucleons act independently is that the parent nucleus will acquire very little recoil momentum and therefore the angular distribution of the evaporation tracks, in the laboratory system will be isotropic.

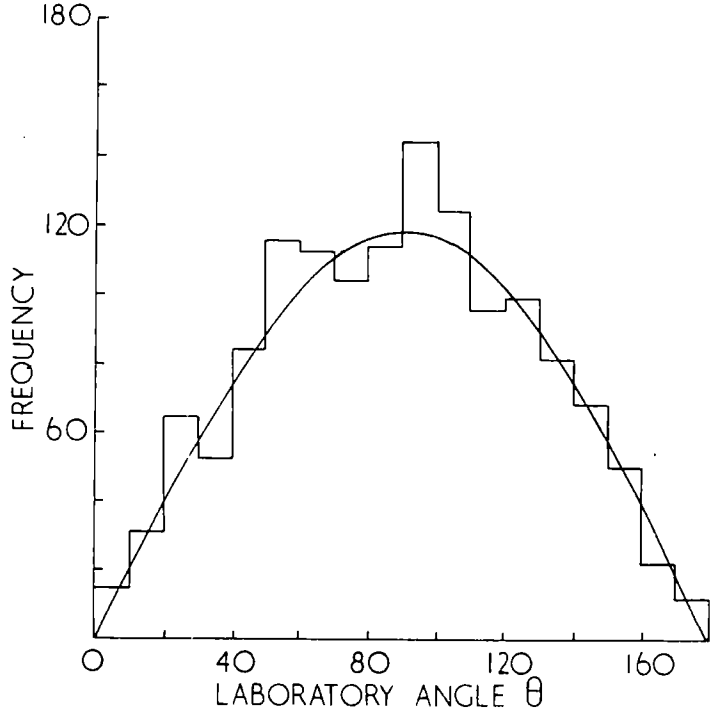

Fig. 35. The angular distribution of black tracks for all events produced by 16·3 Gev. π^--mesons.

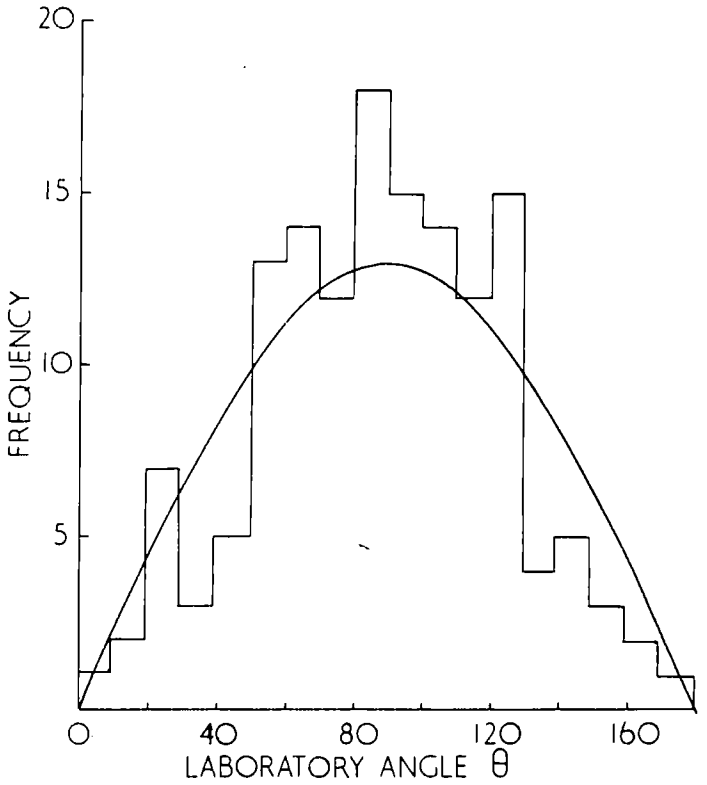

Fig. 36. The angular distribution of black tracks for events produced by 16·3 Gev. π^--mesons with $n_g = 0$.

Figures 35 and 36 show the angular distribution of black tracks for all events and events with $n_g = o$. In each case the expected curve, for an isotropic distribution, is given. The angular distribution is isotropic in both cases confirming that the nucleons act independently.

CHAPTER 4

Long Range Interactions

4.1 Interactions between π-mesons and the Coulomb field of the nucleus Good & Walker 1962a

At large values of momentum, the total energies of particles with different masses but with the same momentum become almost identical. The difference in total energy of two particles of mass M and M^X at momentum p ($pc \gg M$ and M^X) is given by

$$\Delta W = (M^{X2} + p^2)^{\frac{1}{2}} - (M^2 + p^2)^{\frac{1}{2}} = \frac{M^{X2} - M^2}{2p} \quad \ldots\ldots \text{16}$$

By the uncertainty principle the mass M can exist in the state of mass M^X for a time $\Delta t \sim \frac{\hbar}{\Delta W}$ and during this time the particle will travel a distance of the order of $c\Delta t = 2pc\hbar/(M^X - M^2)$. This process may be observed if this transition takes place close to a large body such as a nucleus. In these circumstances momentum can be conserved and the nucleus acquires a small momentum $\Delta p = (M^{X^2} - M^2)/2p$, and an energy $\frac{\Delta p^2}{2M}$ which is also very small. This small momentum transfer can take place by an interaction with the coulomb field. For momentum transfers of the order of 20 MeV/c the intermediate state can exist long enough to travel distances $\sim 10^{-12}$ cm.

It is possible to interpret the phenomenon of bremsstrahlung or pair production in this way. In the case of bremsstrahlung or pair production the intermediate states are, $e \rightarrow e + \gamma$ and $\gamma \rightarrow e^+ + e^-$. Other elementary particles can also exhibit the same properties. In the case of the negative π-meson, the process $\pi^- \rightarrow \bar{p} + n$ might occur if the π^--meson has very high energy.

Table 1 shows a list of processes which may follow this scheme (Good & Walker 1960a).

TABLE 1

	Reaction	Threshold in C Gev.	Threshold in Pb Gev.
1.	$\pi \rightarrow 2\pi$	0.5	1.2
2.	$\pi \rightarrow 3\pi$	1.3	3.3
3.	$\pi \rightarrow K + \bar{K}$	8	21
4.	$\pi \rightarrow K + \bar{K} + \pi$	11	27
5.	$\pi \rightarrow p + \bar{n}$	29	74
6.	$\pi \rightarrow \Sigma + \bar{\Lambda}^o$	45	114
7.	$K \rightarrow K + 2\pi$	1.3	3.3
8.	$K \rightarrow K + 2\pi$	3.0	8.0
9.	$K \rightarrow K + K + \bar{K}$	17	43
10.	$K^+ \rightarrow \bar{\Sigma}^- + n$	39	100
11.	$K^+ \rightarrow \bar{\Xi} + \Lambda^o$	54	138
12.	$\mu^+ \rightarrow \beta^+ + \nu$	8	22
13.	$\mu^+ \rightarrow \pi^+ + \nu$	0.18	0.32
14.	$p \rightarrow n + \pi^+$	5.4	14
15.	$p \rightarrow p + \pi^o$ $p \rightarrow \Lambda^o + K^+$	14	38

The process $\pi \rightarrow 3\pi$ is a suitable one for investigation with the emulsion technique since the threshold of the reaction is low for all the nuclei of the emulsion and the three secondary particles can all be charged.

Physically the process can be described by the Weizsäker-Williams method. The coulomb field of the nucleus can be considered as a spectrum of photons and the interaction proceeds as $\pi^- + \gamma \rightarrow \pi^- + \pi^+ + \pi^-$. The thresholds given in table 1 have been calculated assuming that the most energetic photon, to be found in the field of a nucleus, has a momentum $q = \hbar/r_o A^{\frac{1}{3}} \simeq m_\pi/cA^{\frac{1}{3}}$, and using the expression $q = (M^{X^2} - M^2)/2P$.

Following the Weizsäcker-Williams method an approximate expression for the cross-section of the processes in table 1, has been derived. The cross-section is given by:-

$$\sigma = \frac{3}{2\pi} Z^2 e^2 \int_{K_{thes.}}^{K_{max}} \sigma_\gamma \frac{dK}{K} \ell n \frac{\gamma m_\pi}{KA^{\frac{1}{3}}} \qquad \ldots\ldots 17$$

where σ_γ is the photo-production cross-section for the process considered and K, the energy of the photon.

The approximate relation is obtained by substituting for σ_γ the term e^2/m^2 and is:-

$$\sigma = \frac{3}{4\pi} \frac{Z^2 e^4}{m^{2-}} \left[\ell n \frac{2(p/m_\pi)}{[(M^X/M_\pi)^2 - (M/m_\pi)^2]A^{\frac{1}{3}}} \right]^2 \qquad \ldots\ldots 18$$

where M^X, is the rest energy of the products; M, the rest energy of the incident particle; m, the rest mass of the lightest product and e, the charge of the target nucleus.

The cross-sections σ, for Carbon and Silver, for the process at 16.3 GeV/c are 0.1 mb and 2.2 mb, respectively.

4.2 Ferretti Tridents

Ferretti (1961) has considered the possibility of pair production of π-mesons when a π-meson interacts with the Coulomb field of a nucleus. He has shown that, for energies of about 10 GeV, the cross-section for the process

$$\pi^- + \text{nucleus} \rightarrow \pi^- + \pi^+ + \pi^- + \text{nucleus}$$

becomes appreciable if the produced π-mesons are formed in a resonant state of ($J = 1$, $T = 1$) with an energy of $4m_\pi$. Ferretti also points out that the cross-section, for the $\pi \rightarrow 3\pi$ process, is dependent upon the π-π interaction and is given by the expression

$$\sigma_{\pi\text{-}3\pi} = 10^{-8} \frac{Z^2}{A^{\frac{1}{3}}} \left(\frac{p}{m_\pi}\right)^2 \sigma_{\pi\text{-}\pi} \qquad \ldots\ldots 19$$

where p is the incident π-meson momentum; Z and A, the atomic and mass numbers of the target nucleus; and $\sigma_{\pi\text{-}\pi}$ the total π-π cross-section of the assumed resonance.

The experimental data on the π-3π process gives information on the magnitude of $\sigma_{\pi\text{-}\pi}$.

4.3 Diffraction Dissociation of π-mesons

The problem of the diffraction of particles by a nucleus has been discussed by Feinberg and Pomeranchuk (1956), and Good and Walker (1960b).

For high momenta the angles of divergence, of the particles involved in a collision, are small. In this case the longitudinal component of the momentum transfer to the target q_{11}, is also small, (see equation 22). For these high energies the relation 20 may be satisfied, where R is the radius of the target, the nucleus inthis case.

$$q_{11} R \ll 1 \qquad \ldots\ldots 20$$

Using the uncertainty principle the dimensions of the region in which the collision takes place is given by the expression 21 and for high

$$r_{eff} = \frac{1}{q_{11}} \qquad \ldots\ldots 21$$

energies r_{eff} becomes very large compared with R. This leads to the conclusion that a collision can take place, within this region, with the nucleus as a whole. However, for the nucleus not to be disrupted the transverse momentum transfer q_1 must satisfy the condition $q_1 \leq m_\pi$. Since the nucleus acts as a whole the scattering and subsequent production of particles can be considered as taking place 'externally' with respect to the nucleus.

As an example, consider the case of a π-meson colliding with a nucleus. The scattered π-meson receives a transverse recoil momentum $q_1 \approx p\theta$ and this can lead to the emission of a π-meson. For small angles the longitudinal momentum transfer is given by,

$$q_{11} = [W_\pi^2 - m_\pi^2]^{1/2} - [(W_\pi - W_\pi')^2 - m_\pi^2]^{1/2} - [W_\pi'^2 - m_\pi^2]^{1/2}$$

$$\approx \frac{m_\pi^2 W_\pi'}{2W_\pi(W_\pi - W_\pi')} + \frac{m_\pi^2}{2W_\pi'} \qquad \ldots\ldots 22$$

If it is assumed that the scattered and created meson energies are of the same order of magnitude then q_{11} is given by,

$$q_{11} \approx \frac{3m_\pi^2}{2W_\pi} \qquad \ldots\ldots 23$$

Evaluating expression 23 for the case of an incident π-meson of 16.3 GeV/c, q_{11} is approximately 4 MeV/c, which will not cause the disruption of the nucleus.

The same process may be interpreted in a somewhat different manner. Consider that the incident π-meson is dissociated into a virtual state consisting of two π-mesons. The difference in energy between the two states is $E = (p^2 + (2m)^2)^{1/2} - (p^2 + m^2)^{1/2}$ which reduces to $E = \frac{3m^2}{2p}$ for large values of p. Using the uncertainty relation this state can exist long enough to travel across a nucleus. If there is differential absorption of these two components then the virtual π-meson state can be brought into existence through the diffraction scattering of the incident particle.

This phenomenon can be compared with the action of a ~~Calcite crystal~~ polaroid in the path of a beam of polarised light. If the plane of polarisation of the light is at 45° to the axis of the crystal then the light which passes through the polaroid will consist of two beams which have their planes of polarisation at right angles, one

component being parallel to the direction of the plane of polarization of the initial beam. The component at right angles to this direction has been brought into existence because of the differential absorption, in two perpendicular directions, of the crystal. It follows then that the semi-transparent nuclei can give rise to this type of interaction.

4.4 Experimental Characteristics of Coulomb and Diffraction Dissociation Events

The characteristics of the Coulomb and Diffraction processes, for negative π-mesons, are:- the only secondaries are three charged π-mesons, the total energies of three secondaries is very nearly equal to that of the incident π-meson, and both the longitudinal and transverse components of the momentum transfer, q, to the target are small.

In practise it is difficult to measure the energies of the secondaries so that it is not possible to check the energy balance or that the momentum transfer is small.

However, the limitation to the momentum transfer is reflected in the angular distribution of the secondaries. It can be shown that

$$\sum \sin \theta_i \lesssim \left(\frac{q_{11}}{q}\right)_{max} \qquad \ldots\ldots 24$$

and substituting for the components of the momentum transfer q

$$\sum \sin \theta_i \lesssim A^{-\frac{1}{3}} \qquad \ldots\ldots 25$$

In section 4.1 it has been shown that the cross-section for the Coulomb process is proportional to Z^2 and so the expected value for $\sum \sin \theta_i$ is determined by the heavier elements of the emulsion, for which the average value of $A^{-\frac{1}{3}}$ is 0.23. Thus $\sum \sin \theta \gtrsim 0.23$.

In section 4.3 it is stated that semi-transparent nuclei are necessary for inelastic diffraction scattering to take place. In chapter 2 it was concluded from the optical model that, at 16 GeV/c, the absorption coefficient K is equal to $(2.4 \pm 0.2) \times 10^{-12} cm^{-1}$. The corresponding transparencies of the heavy and light elements are 17% and 40% respectively. These numbers indicate that inelastic diffraction scattering will be predominant in the lighter nuclei of the emulsion. Carbon is typical of the light elements and for these $\sum \sin \theta_i \gtrsim 0.44$. Events of the Coulomb and Inelastic Diffraction type must satisfy these angular criteria, but it must be pointed out that it is possible for normal inelastic interactions to satisfy these conditions also.

4.5 Experimental

In the 192.5 metres of track which has been followed 13 events of the type (0 + 3) have been observed and analysed. The spatial angles of the secondaries, relative to the primary, have been measured and scattering measurements made on all secondaries long enough to yield a result. Table 2 gives a summary of these results (Table 2 over page).

TABLE 2

Event Nos.	$\sum E$ sec.	E_1 GeV	E_2 GeV	E_3 GeV	θ_1	θ_2	θ_3
214 - 4	(16 ± 4)	(8.1 ± 2.7)	too short	(8.4 ± 3.1)	3° 17'	5° 27'	3° 35'
219 - 13	(5 ± 1)	(3.0 ± 0.8)	(2.2 ± 0.5)	too short	1° 40'	1° 53'	7° 46'
222 - 38	(8 ± 1)	too short	(6.8 ± 1.0)	(1.1 ± 0.5)	9° 48'	1° 28'	7° 20'
222 - 42	(6 ± 1)	(4.0 ± 0.7)	too short	(2.3 ± 0.6)	1° 8'	0° 30'	1° 38'
222 - 44	(3 ± 1.5)	too short	too short	(2.6 ± 1.3)	5° 56'	2° 14'	3° 14'
208 - 55	(2 ± 1)	too short	too short	(2.0 ± 0.9)	22° 39'	1° 40'	2° 47'
208 - 60	(15 ± 3)	(6.3 ± 2.1)	(8.3 ± 2.8)	too short	2° 29'	1° 40'	2° 47'
211 - 23	(14 ± 3)	(5.8 ± 2.3)	too short	(8.1 ± 2.8)	1° 58'	9° 41'	2° 52'
219 - 25	(13 ± 3)	(7.0 ± 1.5)	(6.4 ± 2.7)	too short	1° 43'	0° 37'	7° 34'
217 - 13	(17 ± 3.5)	(9.6 ± 3.3)	(7.6 ± 1.2)	too short	1° 24'	0° 36'	6° 37'
215 - 1	h i g h	l o c a l	d i s t o r t i o n		4° 18'	5° 17'	1° 3'
215 - 7	(12 ± 3)	too short	(8.1 ± 2)	(4.3 ± 1.5)	6° 58'	0° 30'	9° 20'

Events of this type in which three charged secondaries are produced arise in three ways,

(i) the processes discussed in the previous sections,

(ii) by the reactions in nuclei

$$\pi^- + n \rightarrow p + \pi^- + \pi^-$$

$$\pi^- + n \rightarrow \Sigma^- + K^+ + \pi^-$$

in which momentum is approximately balanced and the excitation energy of the nucleus being lost in the form of evaporation neutrons. Also

(iii) by the inelastic nuclear interaction.

π^- + nucleus → final nucleus + 3π + other neutral secondaries, in which momentum is not balanced amongst the charged secondaries.

By visual inspection one of the events has been classified as an inelastic nuclear interaction and consequently rejected.

From table 2 it can be seen that it has not been possible to make complete momentum measurements for any of the 12 other events. Consequently it has not been possible to check any event for momentum balance or small transverse momentum transfer. However, 7 of the 12 events have been rejected since it is not possible to conserve both momentum and total energy with the measured spatial angles of the produced π-mesons. Events of the coulomb or inelastic diffraction type have momentum vectors described by the equations,

$$p_1 \ell_1 + p_2 \ell_2 + p_3 \ell_3 = 16.3 - qx$$

$$p_1 m_2 + p_2 m_2 + p_3 m_3 = - qy$$

$$p_1 n_1 + p_2 n_2 + p_3 n_3 = - qz \qquad \ldots\ldots 26$$

where p_1, p_2 and p_3 are the momentum vectors and ℓ, m and n the direction cosines of the three produced mesons. qx, qy and qz are the components of the momentum transferred to the nucleus. Since these are of the order of a few MeV they can be neglected with respect to the other quantities thus enabling the equations to be solved simultaneously, giving values for p_1, p_2 and p_3. Now since these components of momentum are of the order of a few GeV/c the total energy for the case of 3π-meson secondaries is given numerically by $\Sigma|p_i|$. Thus any event which does not satisfy the relation $\Sigma|p_i| = 16.3$ can be rejected.

The result of the computation is that 7 of the events can be fitted only if one or more of the values of momentum are negative (i.e. the secondary travels in the opposite direction to its observed direction). These events are excluded. The remaining five events which are shown in Table 3 all satisfy $\Sigma|p_i| = 16.3$ GeV. It is emphasised that this is a rejection technique. The events satisfying the equations are not necessarily of the coulomb or inelastic diffraction type. It is possible that the measured angles fortuitously satisfy the equations. The measured values of p_1 are shown in Table 3 for comparison.

TABLE 3

Event No.	p_1 GeV/c	p_2 GeV/c	p_3 GeV/c	$\Sigma\|p_i\|$ GeV/c
214 - 4	9.235	3.738	3.366	16.338
Observed	(4.0 ± 1.0)	(0.8 ± 0.4)	(1.5 ± 0.5)	
219 - 25	7.691	6.101	2.538	16.330
Observed	(5.3 ± 0.6)	(4.8 ± 1.2)	too short	
211 - 23	9.496	1.378	5.459	16.333
Observed	(4.3 ± 0.6)	too short	(3.4 ± 0.8)	
217 - 13	5.487	9.216	1.610	16.313
Observed	(2.5 ± 0.5)	(8.1 ± 1.6)	too short	
216 - 4(1+3)	4.283	2.623	9.459	16.365
Observed	4.7 ± 1.2	too short	(4.6 ± 1.8)	

Table 4 shows the results of the rejection technique as applied to accepted events, from the results obtained by the CERN emulsion group (Baldassarre et al. 1961). The measured momenta are also given for comparison.

TABLE 4

Event Nos.	p_1 GeV/c	p_2 GeV/c	p_3 GeV/c	$\Sigma\|p_i\|$ GeV/c
21 - 42	3.00	10.836	0.153	13.989
Observed p	6.8	6.7	0.7	14.2
21 - 50	-8.125	17.087	5.048	30.260
Observed p	0.7	7.0	0.8	8.5
125 A	9.80	4.12	0.086	14.006
Observed p	5.8	8.8	0.41	15.01
146 A	3.95	6.19	3.93	14.07
Observed p	2.70	6.10	3.10	11.90
142	0.65	5.04	8.33	14.02
Observed p	0.63	?	5.40	?

The technique rejects one event from the CERN results which is acceptable from the measured momenta.

The five events, from this laboratory, have been subjected to further analysis in terms of the reactions,

$$\pi^- + n \rightarrow p + \pi^- + \pi^-$$

$$\pi^- + n \rightarrow \Sigma^- + K^+ + \pi^-$$

Each secondary has been classed as ϵ, K or π in turn. In the most favourable case the interaction would have an associated excitation energy of 450 MeV which is lost in the form of evaporation neutrons. This energy is too large to be considered as being lost solely as evaporation neutrons.

These five events are now clearly coulomb or inelastic diffraction events or inelastic nuclear interactions in which momentum is fortuitously balanced. To obtain further evidence on this point 38 known inelastic events of the type $(n_h + 3)\pi$ have been analysed in this way. In one event only, of the type $(1 + 3)\pi$, it is possible to conserve both momentum and total energy. Since the heavy track is short and of low energy it is possible that this event is of the coulomb or inelastic diffraction type. This then probably eliminates the possibility that these five events are of type (iii) leaving only the type (i).

Fig. 37 shows the distribution of $\sum \sin \theta_i$ for the 12 events from this laboratory together with the 13 events from the CERN group.

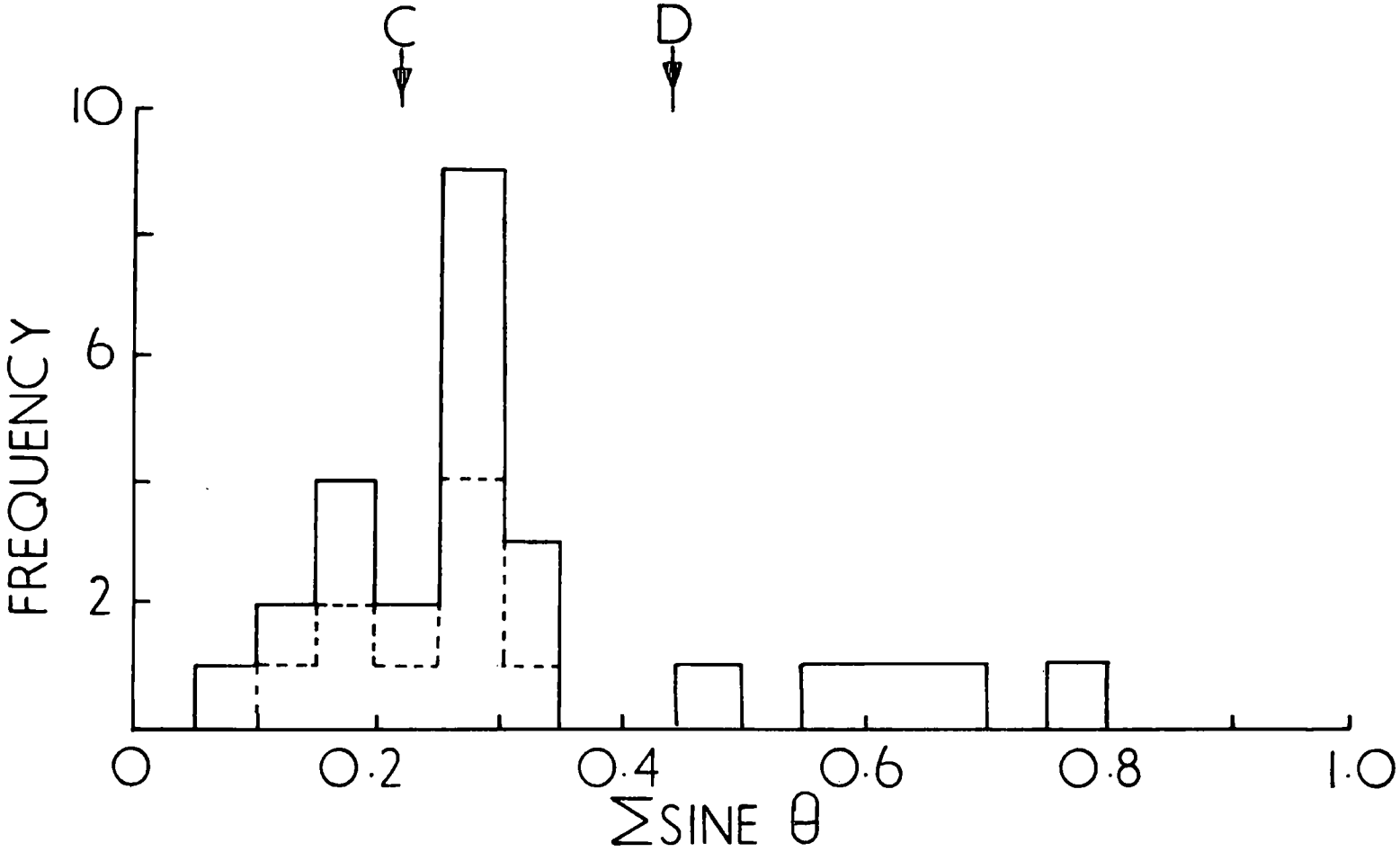

Fig. 37. The distribution of Σ sine θ. —— All 'tridents'.
----- Tridents with momentum balance.

The arrows marked C and D represent the expected position of the maximum values of $\sum \sin \theta$ for Coulomb and Diffraction events respectively. The dotted line is the distribution of events not rejected by the simultaneous equation technique. The events fall within the region of the inelastic diffraction process, but close to the acceptable region for the Coulomb process.

However, assuming that the events, from this laboratory, are from the Coulomb process, they have been treated as Ferretti 'tridents' and the mass M^X of the resonant state has been calculated on the basis that the two π-mesons of lower momenta are the products of the resonant state. The results are given in table 5.

TABLE 5

Event Nos.	M^X MeV/c^2
214 - 4	380
219 - 13	707
211 - 23	536
217 - 13	610
216 - 4	695
Mean	586 $\pm$ 60

This value is consistent with the value of M^X predicted by Ferretti i.e. $4m = 560$ MeV. The two other possible combinations of π-mesons give mean values of 740 and 770 MeV/c^2.

4.6 Conclusions

In both the Coulomb and Diffraction processes the energy required to form the new mass state of the pion is the same and the limitations to the momentum transfer are very similar. Differences arise from the fact that the Coulomb process occurs predominantly from collisions with heavy nuclei, whereas the Diffraction process occurs with less opaque light nuclei. The evidence of this laboratory, together with that of the CERN group, indicates that the process π + nucleus $\rightarrow 3\pi$ + nucleus exists but that the nature of the process is uncertain.

Assuming then that the five non-rejected events occur when the incident π^--meson interacts with the heavy nuclei in the emulsion, the mean free path is 25.9 metres after correcting for contamination of the beam. This corresponds to a cross-section $\sigma_{\pi-3\pi} = 18.9$ mb which is necessarily an upper limit.

From equation 1 it follows that if the process occurs as described by Ferretti then the upper limit to the π-π cross-section is given by $\sigma_{\pi-\pi} = 66.4\ \sigma_{\pi-3\pi} = 1252$ mb at the (J = 1, T = 1) resonance. The mass of the state is (586 ± 60) MeV/c^2.

Doubt is cast on this result, however, since all possible combinations of the secondaries give values of M^x of the same order of magnitude and close to the expected value.

Moreover, the distribution of $\sum \sin \theta$ shows that those events, which are not rejected on conservation of momentum grounds, satisfy the condition $\sum \sin \theta < 0.44$, i.e. the condition for inelastic diffraction scattering. The condition for coulomb dissociation, $\sum \sin \theta < 0.22$ is not completely satisfied by this group of events. Taking the CERN results together with those of this laboratory, a total of 26 tridents with 3 secondary π-mesons have been observed and of these 9 satisfy the conditions for inelastic diffraction scattering i.e. 35% of the trident events.

This result is consistent with that of Bellini et al. (1962) where a study of tridents produced by 18 GeV π^--mesons in a heavy liquid bubble chamber shows that 30% of the tridents satisfy the conditions for inelastic diffraction scattering.

CHAPTER 5

Conclusions

In the preceding chapters the inelastic interactions, Coulomb Dissociation and Inelastic Diffraction scattering of π^--mesons have been studied.

Inelastic Interactions

The angular distribution of minimum tracks does not show the spectrum of target masses as suggested by the results of Friedlander (1960). Taking all events together the distribution of $\overline{\ell n \cot \theta}$ does not agree with the distributions calculated by Castagnoli et al. (1953) and Duller and Walker (1954). The experimental distributions are much broader than the calculated distributions. The deviations from the calculated distributions have been explained in terms of secondary collisions and the effect of the continuing primary and the momentum distribution in the centre of mass system. The effect of secondary collisions is to give values of $\ell n\ \gamma_c$ which are lower than the expected value whereas the effect of the continuing primary is to give values of $\ell n\ \gamma_c$ which are larger than the expected value.

A method of selecting interactions due to single collisions between the π^--meson and a nucleon has been developed. The method does not follow the usual practice of dividing the events into those occurring in light and heavy nuclei, nor are the events selected on

the basis of n_h being very small. In fact it is the number of grey tracks which gives a better indication of the number of collisions taking place inside a given nucleus. The result of the method is that those events with $n_g = o$ are due to interactions in which only one collision has occurred. These events show clearly an excess of particles emitted at small angles which is expected on the basis of the effect of the continuing primary. The correction for the continuing primary brings agreement between the experimental and calculated angular distributions of Castagnoli et al. (1953) and Duller and Walker (1954).

Agreement between the calculated distributions and the experimental angular distribution of minimum tracks has also been found for events with $n_g = 1$. A comparison of the present data and that obtained by Goldsack (1962) for the interactions of 16.3 GeV π^--mesons with protons indicates that one third of the events with $n_g = 1$ are probably single collision events. Furthermore the group of events with $n_g = 1$ have a slightly larger evaporation energy than is expected for single collisions. Consequently the selection of single collision events on the criterion of $n_g = o$ will lead to a more pure sample of events than taking those with $n_g = o$ and 1 but a detailed study of single collisions will suffer by the omission of events in which the recoil proton is slow.

For some time it has been realised that events with large numbers of black tracks are events in which more than one collision has occurred within a nucleus but until now it has not been possible to relate the number of collisions to the observed number of black tracks. In the present work a relation between the number of collisions and the evaporation energy has been derived. Comparison of this relation with the experimental results shows that it explains the general features but is not correct in detail, the detailed discrepancy being inevitable while neutral particles cannot be detected. It can be concluded, however, that the evaporation energy is closely related to the number of nucleons removed from the nucleus.

From the observed average number of grey tracks the average cross-section for interaction of the secondary particles has been estimated and is in good agreement with the average of the measured total cross-sections for the interaction of protons and π-mesons with nucleons. The relation between the number of grey and minimum tracks derived on the basis of several quasi-independent collisions is also in good agreement with the experimental results.

Coulomb and Diffraction Dissociation of π^--mesons

The selection criteria for Coulomb and Diffraction Dissociation of π^--mesons are very similar. If these processes occur it is expected to find that Coulomb Dissociation will occur in the electric field of the heavy nuclei and Diffraction Dissociation in

the nuclear field of the light nuclei of the emulsion. In each case the target nucleus must act coherently and consequently there are different upper limits to momentum transfer to the nucleus in each case. On the basis of this alone those events in which it is possible to conserve momentum with the measured angles have been classified as Diffraction Dissociation. The events of this laboratory taken with that of the CERN group show that 35% of all tridents are due to the Diffraction Dissociation process which is in fair agreement with the result of 30% obtained by Bellini et al. It has been concluded from the present data that there are two types of inelastic nuclear interactions, one in which the nucleons act independently, inelastic scattering; and one in which the nucleons act coherently; inelastic diffraction scattering.

ACKNOWLEDGMENTS

The author wishes to thank Professor G.D. Rochester for his constant interest in this work. He also wishes to thank Dr. Major and Dr. Apostolakis for their collaboration and his other colleagues for assistance in various stages of the work. His thanks go also to CERN for arranging and making the exposure of the plates. Finally, he wishes to thank DSIR and NATO for maintenance grants during the work.

REFERENCES

Allen, J.E., Apostolakis, A.J., Lee, Y.J., Major, J.V., and Perez, Ferreira, E.,
1959, Phil. Mag., 4, 858.

Allen, J.E., Apostolakis, A.J., Lee, Y.J., Major, J.V., and Perez Ferreira, E.,
1961, Phil. Mag., 6, 833.

Ashmore, A., Cocconi, G., Diddens, A.N. and Wetherall, A.M.,
1960, Phys. Rev. Lett., 5, 576.

Atkinson, J.H., Hess, W.N., Perez-Mendez, V., and Wallace, R.W.,
1959, Phys. Rev. Lett., 2, 168.

Baldassarre, F., Caforio, A., Ferraro, D., Ferilli, A., Merlin, M., Perkins, D.H., Semeraro, S., Combe, J.C., Gibson, W.M., Lock, W.O., Bonetti, A., DiCorato, M., Fedrighini, A., Hertz, A.J., Sichirollo, A.E., Tallone, L., Vegni, G., and Villar, E.,
1961, Nuovo Cimento, 21, 459.

Barbaro, Galtieri, A., Baroni, G., Manfredini, A., Castagnoli, C., Lamborizio, C., and Ortalli, I.,
1961, Nuovo Cimento, 21, 487.

Bellini, G., Fiorini, E., Herz, A.J., Negri, P., Ratti, S.,
1962 Proceedings of the Rochester Conference, 613.

Blau, M., and Caulton, M.,
1954, Phys. Rev., 96, 150.

Bogachev, N.P., Fen, V.S., Gramenitskii, J.M., Kirilova, L.F., Lebedev, R.M., Liubimov, V.B., Markov, P.K., Merekov, Iu. P.P., Podgortakii, M.I., Sidorov, V.M., Tolstov, K.D., Tolstov, K.D., and Shafranova, M.G.,
1958, Sov. Journ. of Atomic Energy, 4, 373.

Bozoki, G., Fenyves, E., Frenkel, A., Gombosi, E., and Suranyi, P.,
1962, Nuovo Cimento, 24, 29.

Brieman, C., Caejthey-Barth., Lagnaux, J.P., and Sacton, J.,
1961, Nuovo Cimento, 20, 1017.

Castagnoli, C., Cortini, G., Franzinetti, C., Manfredini, A., and Moreno, D.,
1953, Nuovo Cimento, 10, 1539.

Cavanaugh, R.E., Haskin, D.M., and Schein, M.,
1953, Phys. Rev., 100, 1263.

Ciok, P., Danysz, M., Gierula, J., Jurak, A., Miesowicz, M., Perneger, J., Vrana, J., and Wolter, W.,
1957, Nuovo Cimento, 6, 1409.

Ciok, P., Coghen, T., Cierula, J., Holynai, R., Jurak, A., Miesowicz, M., San ieivska, T., and Perneger, J.,
1958, Nuovo Cimento, 10, 741.

Coor, T., Hill, D.A., Hornyak, N.F., Smith, L.W., and Snow, G.,
1955, Phys. Rev., 98, 1369.

Crew, J.E., and Hill, R.D.,
1958, Phys. Rev., 110, 177.

Cuilli, I., Glagolev, V.V., Nikitin, V.A., Petrizilka, V.,
Sviridov, V.A., and Tolstov, K.D.,
1962, Nuovo Cimento, 25, 1197.

Duller, N.M., and Walker, W.D.,
1954, Phys. Rev., 93, 215.

Edwards, B.P., Engler, A., Friedlander, M.W., and Kamal, A.A.,
1957, Nuovo Cimento, 5, 1188.

Feinberg, E.L., and Pomeranchuk, I.,
1956, Suppl. Nuovo Cimento, 3, 652.

Fernbach, S., Serber, R., and Taylor, T.B.,
1949, Phys. Rev., 75, 1352.

Ferretti, B.,
1961, Nuovo Cimento, 19, 193.

Friederlander, E.M., Marcu, M., and Spirchez, M.,
1960, Nuovo Cimento, 18, 623.

Finney, P.J., Major, J.V., Parkhouse, P.G.J.T.,
1962, Phil. Mag., 7, 237.

Gierula, J., Miesowicz, M., and Zielinski, P.,
1960a, Acta Physica Polonica, 19, 119.

Gierula, J., and Miesowicz, M.,
1960b, Nuovo Cimento, 18, 102.

Gierula, J.,
1960c, Proceedings of the Rochester Conference, 816.

Goldsack, S.J., Riddiford, L., Tallini, French, B.R., Neale, W.W., Norbury, J.R., Skillicorn, I.O., Davies, W.T., Derrick, M., Mulvey, J.H., and Radojicic, D.,
1962, Nuovo Cimento, 23, 941.

Gooding, T.J., and Pugh, H.G.,
1960, Nuclear Physics, 18, 46.

Good, M.L., and Walker, W.D.,
1960a, Phys. Rev., 120, 1855.

Good, M.L., and Walker, W.D.,
1960b, Phys. Rev., 120, 1857.

Grote, L.C., Krecker, V., Lanius, K., Manske, G., and Meier, H.W.,
1961, Nuclear Physics, 34, 1676.

Heisenberg, W.,
1962, Zeits. Phys., 133, 65.

Johnson, W.R.,
1955, Phys. Rev., 100, 1263.

Kalbach, R.M., Lord, J.J., and Tsao, C.H.,
1959, Phys. Rev., 113, 330.

Kraushaar, W., and Marks, L.J.,
1954, Phys. Rev., 93, 326.

Landau, L., and Belenky, S.Z.,
1956, Suppl. Nuovo Cimento, 3, 15.

Le Couteur, K.J.,
1950, Proc. Phys. Soc., 63, 498.

Lees, C.F., Morrison, G.C., Muirhead, H., Rosser, W.G.V.,

1953, Phil. Mag., 44, 304.

Longo, M.J., and Moyer, B.J.,

1962, Phys. Rev., 125, 701.

Lock, W.O., March, P.V., Muirhead, H., and Rosser, W.G.V.,

1955, Proc. Roy. Soc., A230, 215.

Lykhachev, M.F., Stanvisky, V.S., Yun-Chang, H., and Nai-sen, C.,

1962, Soviet Physics, 14, 29.

Pugh, H.G., and Riley, K.F.,

1961, Proceedings of the Rutherford Conference, 195.

Peacock, R.N., Haln, B., Hugentobler, E., and Steinrisser, F.,

1961, Nuovo Cimento, 22, 1290.

Skyrme, D.M.,

1962, Nuclear Physics, 35, 177.

Takagi, S.,

1952, Prog. Theor. Phys., 7, 123.

Winzeler, H., Klaiber, B., Koch, W., Nicolic, M., and Schneeberger, M.,

1960, Nuovo Cimento, 16, 8.

Wikner, F.,

1957, Ph.D. Thesis.

Zhdanov, G.N., Maksimenko, M.N., Tret'Yakora, M.I., and Shcherbakova, M.N.,

1960, Soviet Physics, 10, 442.

APPENDIX A.1

The Processing of the 600μ Plates Exposed to the 16.3 GeV Negative π-meson Beam

After the grid has been put on each pellicle the pellicles are stuck down centrally on treated glass sheets 32 cm x 16 cm. The treated glasses have been soaked in a solution of 49% distilled water, 49% alcohol, 2% glycerine and a few drops of a wetting agent. A plate is selected if an unbroken film of liquid covers the surface. Any imperfection in the film of liquid covering the plate can cause bubbles to appear on a plate during the processing of the stuck down pellicles. The selected plate is then laid flat and one surface of the emulsion quickly wetted with the solution. The emulsion is laid, wet face downwards, on the glass plate and the emulsion is then rolled with a squeegee from which several kilograms weight is hung. The sticking down must be completed before the solution penetrates and softens the emulsion. The whole procedure is therefore carried out at a low temperature. The plates are placed on each other under a weight of several kilograms and left for at least 12 hours in order to dry out.

Before starting the processing of the plates they are placed in a dry enclosure at 5°C and then the plates are allowed to soak in water for $2\frac{1}{2}$ hours. This enables the developer to penetrate more quickly in the following stage. From the pre-soak the plates are placed in the

developer, the composition of which is given at the end of this appendix, at 5°C and allowed to soak for a further $2\frac{1}{2}$ hours. This enables a uniform distribution of developer to be obtained in the emulsion with no development.

The plates are removed from the cold developer after the $2\frac{1}{2}$ hours soak is complete and the excess developer is removed. The plates are then put into the hot stage which is set at 17°C where development takes place, and are left for $1\frac{1}{2}$ hours.

The development is stopped by putting the plates into a washing solution which is at 5°C, for a period of 3 hours.

Fixing takes place in the 30% hypo solution at 5°C and as the plates fix so they become clear. This takes approximately 84 hours. The fixing solution is replenished regularly with fresh hypo during fixing. The replenishing solution contains 2% of sodium sulphate which hardens the emulsion and reduces swelling and bubbling.

When the plates are clear the fixing solution is slowly reduced in concentration, over a similar period as is taken to fix i.e. 84 hours, to 0.1%. At this stage direct washing is substituted until the test for hypo with potassium permanganate gives a negative result. Finally the plates are soaked in a 2% glycerine solution at 5°C for $2\frac{1}{2}$ hours. This plasticises the emulsion and reduces the strains when drying. The plates are blotted and dried at room temperature by blowing air over them with a small fan. The drying takes about 12 hours during which time the emulsion shrinks to half its original thickness. The dry plates have a surface fog and this is cleaned off

with a little alcohol.

Solutions used for processing

Developer = 18 gm Sodium Sulphite

0.8 gm Potassium Bromide

4.5 gm Amidol

The chemicals are dissolved in distilled water and made up to 1 litre, filtered and cooled to 5°C. The pH of the solution is adjusted to 6.8 with a solution of potassium metabisulphite (85 gm to 320 cc of distilled water).

Wash:- A solution of 18 gm of Sodium Sulphite to 1 litre of distilled water. The pH is again adjusted to 6.8.

Fixer:- 300 gm Hypo

25 gm Potassium metabisulphite

12 gm Silver Bromide

The chemicals are dissolved in distilled water and made up to 1 litre, filtered and cooled to 5°C.

APPENDIX A.2.

Star size distributions

All events

N_s \ N_g	0	1	2	3	4	5	6	7	8	9	10	11	12	
0		3	3			1								7
1	40	4	3				1							48
2	13	14	3		1	1			1					33
3	32	10	6		3	2	1							54
4	13	18	6	3	3	2	1	3						49
5	23	7	5	5	4	2	2	1	1					50
6	11	8	4	2	2	2	2	1	1					33
7	8	9	3	5	3	3	1	2	2		1			37
8	4	8	5	1		2	3	1						24
9	2		2	2	3	3	4							16
10		2	1										1	4
11		1	2	1			2	1						7
12		1	1	1	1		1							5
13	1	1	1		1	1	1							6
14				1										1
	147	86	45	21	21	19	19	9	5		1		1	374

All events

N_b \ N_g	0	1	2	3	4	5	6	7	8	9	10	11	12	13	14	
0	76	15	2		2											95
1	25	12	5	1												43
2	12	10	6	3	3											34
3	12	11	2	4	1		1									31
4	14	7	2			1	2									26
5	5	7	3	1	1	1	1									19
6	1	4	5	1		1		3	2							17
7		4	5	1	1	1										12
8	1	3	3	1	2	3	1		1							15
9	1	2	1	2		1	1		1							9
10		1	6	2	2	2		2	1		1					17
11		2	2		3	1	2	1					1			12
12				4	1	3		1								9
13		3			1	2	4									10
14		2			1		2									5
15		1	1		2	1	1									6
16		1					1	1								3
17			1	1	1	1	1									5
18		1					1									2
19							1									1
20						1		1								2
21																
22		1														1
	147	86	45	21	21	19	19	9	5		1		1			374

All events

N_b \ N_s	0	1	2	3	4	5	6	7	8	9	10	11	12	13	14	
0	1	23	10	16	11	16	9	6	3							95
1	1	15	5	8	7	3		1	1	2						43
2	1	3	4	10	5	5	2	1	1		1		1			34
3		2	3	4	3	4	7	5		1		1		1		31
4	1	2	3	6	4	4	2	1	2					1		26
5		1	1	5	1	2	2	2	3	1		1				19
6			2		5	2	4	3	1							17
7		1	1	1	3	1		2	1	1	1					12
8			1		1	4		2	3		1					15
9	1		3			1		2	1						1	9
10	2			2	3	3	1	3	1	1		1				17
11					3	2	2		3	1	1					12
12				1		2	1	2	1	1		1				9
13						1	1		2	1		1	1	3		10
14							1	2				1	1			5
15				1			1	1		1			1	1		6
16								2	1							3
17					1			2		2						5
18		1			1											2
19													1			1
20					1					1						2
21																
22												1				1
	7	48	33	54	49	50	33	37	24	16	4	7	5	6	1	374

Events with $N_g = 0$

N_b \ N_s	0	1	2	3	4	5	6	7	8	9	10	11	12	
0		23	9	13	6	14	7	2	2					76
1		11	2	6	2	2		1	1					25
2		3	1	5	1	1		1						12
3		1		1	1	2	3	3				1		12
4		1	1	6	3	2			1					14
5		1		1		1		1		1				5
6							1							1
7														
8						1								1
9									1					1
		~~17~~ 40	13	32	13	23	11	8	4	2		1		~~124~~ 147

Events with $N_g = 1$

N_s / N_b	0	1	2	3	4	5	6	7	8	9	10	11	12	13	
0	1		1	2	6	1	2	2	1						16
1	1	2	3	1	3	1			1						12
2			2	3	2		1	1			1				10
3		1	2	3	1	1	1	1				1			11
4	1		2		1		1		1						6
5			1	1	1		2	1	1						7
6					1	2	1	1							5
7			1		1			1							3
8			1		1				1		1				4
9			1												1
10				1											1
11					1	1									2
12															
13									1				1	1	3
14							1		1						2
15								1							1
16								1							1
17															
18		1													1
	3	3	14	11	18	6	9	9	7		2	1	1	1	86

Events with $N_g = 2$

N_s / N_b	0	1	2	3	4	5	6	7	8	9	10	11	12	13	
	X		X	X		X		X							X
0						1		1							2
1		2		1						1					4
2	1			3	±	1	1								6
3			1				1								2
4					1	1								1	3
5				1		1			1						3
6			2		1		1		1						5
7		1		1	1				1		1				5
8						1		1		1					3
9								1							1
10	2				2			1			1				6
11							1		1						2
12															
13															
14															
15													1		1
16															
17					1										1
18															
19															
20															
21															
22															
23												1			1
	3	3	3	6	6	5	4	4	2	2	1	1	1	1	45

APPENDIX A.3.

Duller and Walker Plots for events with n_s = 1 to 14.

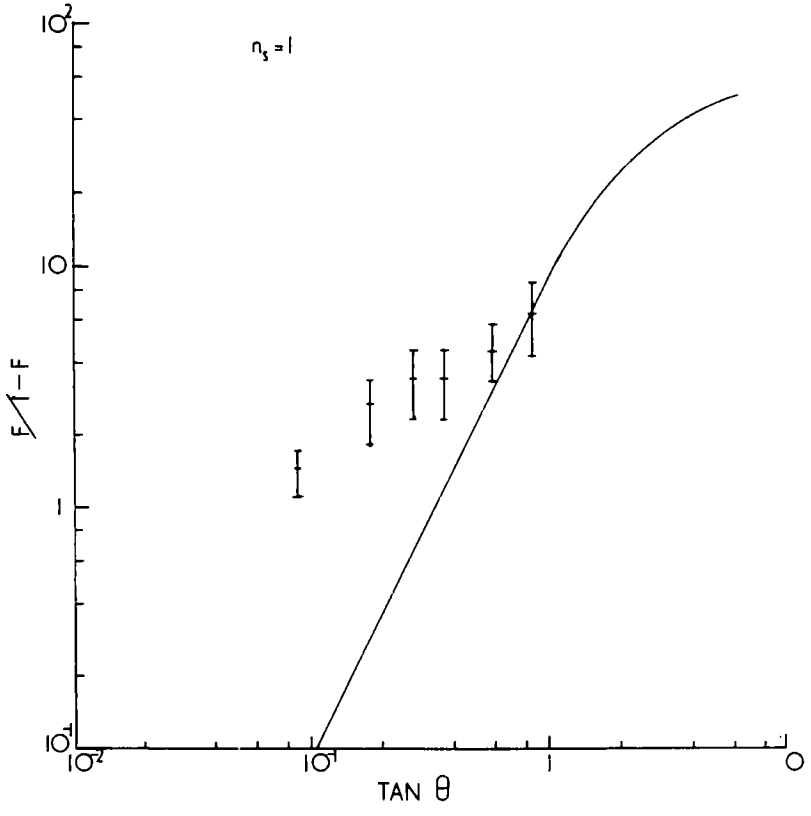
$n_s = 1$
10^2
10
1
10^{-1}
10^{-2}
10^{-1}
1
0
F/1-F
TAN θ
Fig.38.

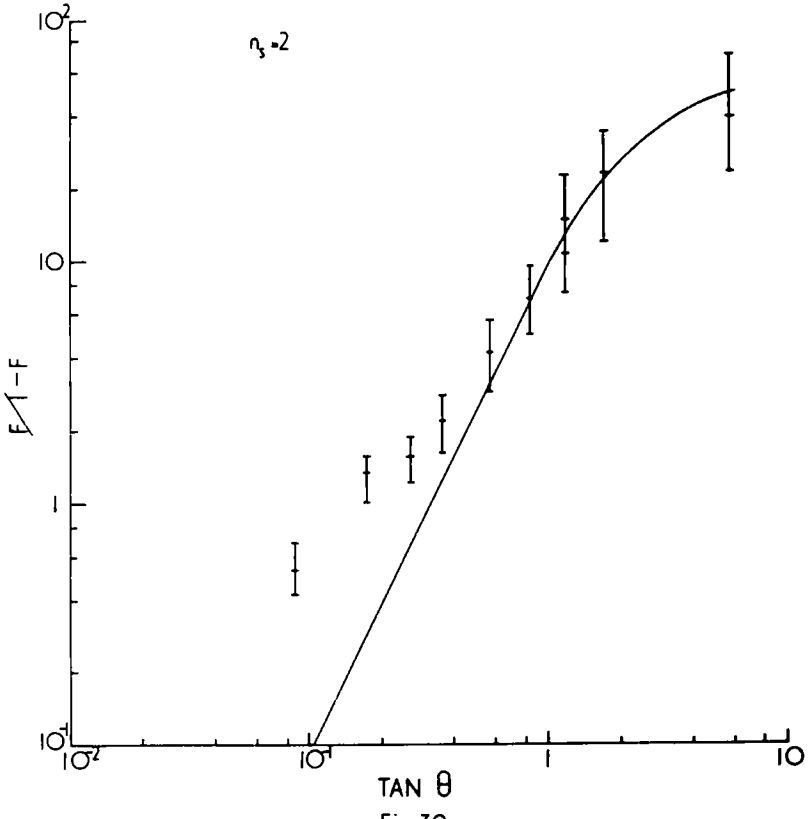
$n_s = 2$
10^2
10
1
10^{-1}
10^{-2}
10^{-1}
1
10
F/1-F
TAN θ
Fig.39.

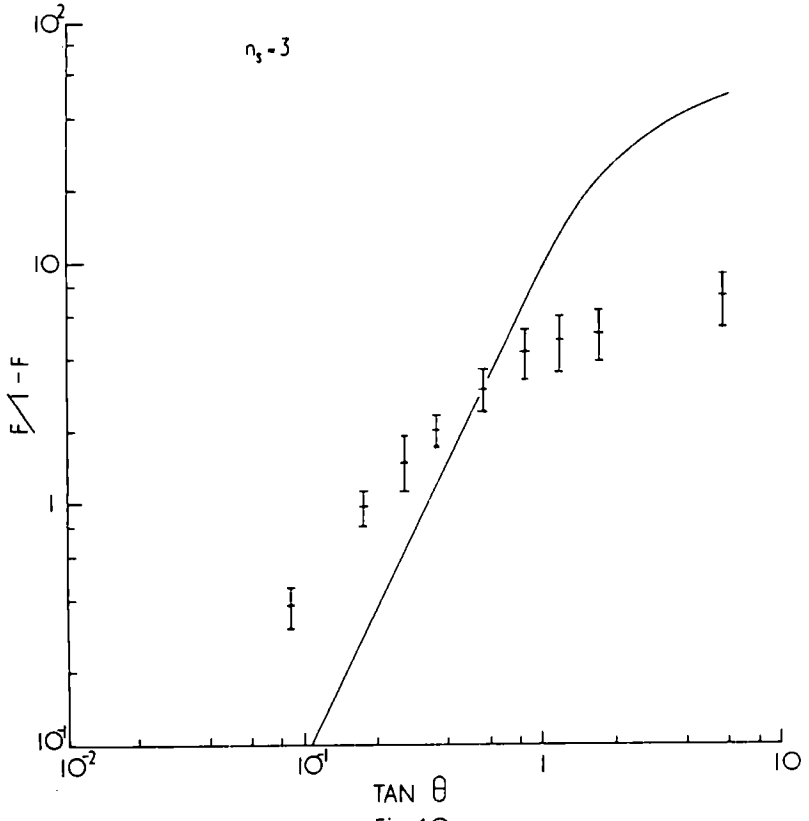
$n_s = 3$
10^2
10
1
10^{-1}
10^{-2}
10^{-1}
1
10
E/1 - F
TAN θ
Fig. 40.

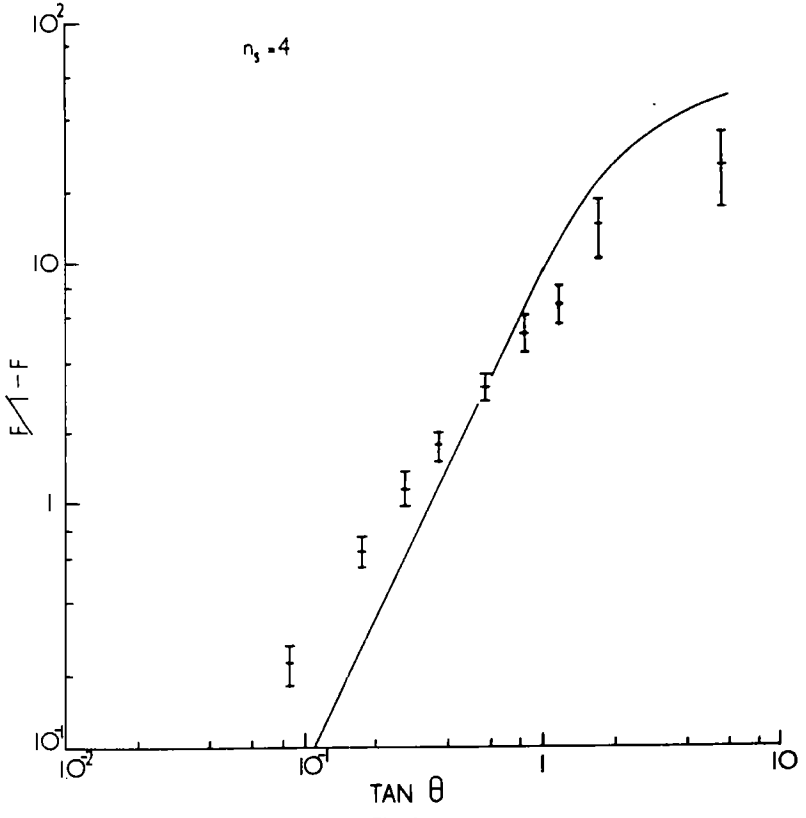
$n_s = 4$
10^2
10
1
10^{-1}
10^{-2}
10^{-1}
1
10
E/1 - F
TAN θ
Fig. 41.

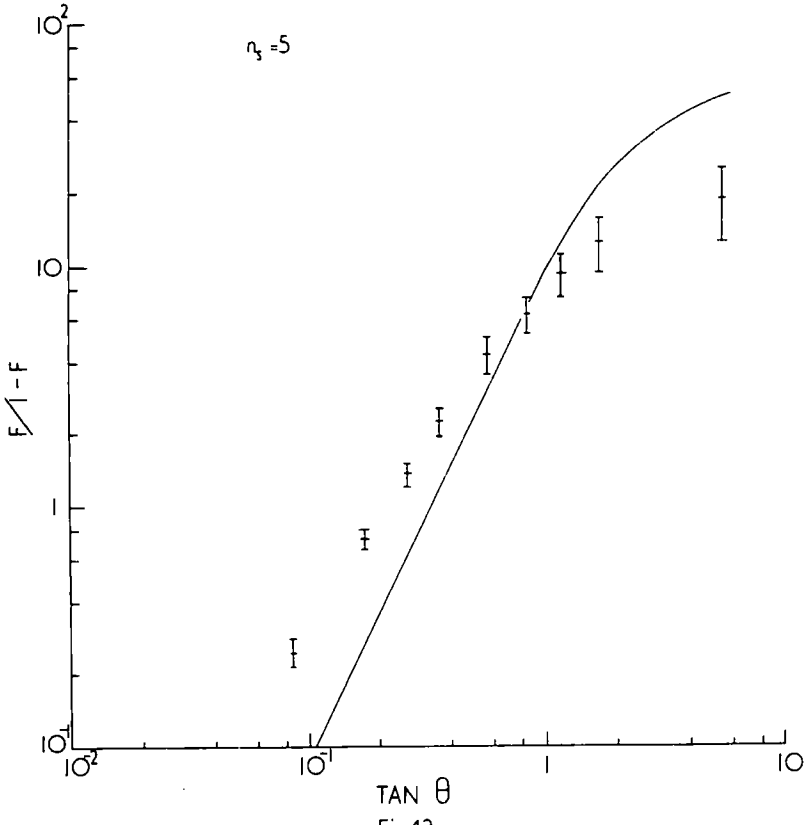
$n_s = 5$
10^2
10
1
10^{-1}
F/1 - F
10^{-2}
10^{-1}
1
10
TAN θ
Fig.42.

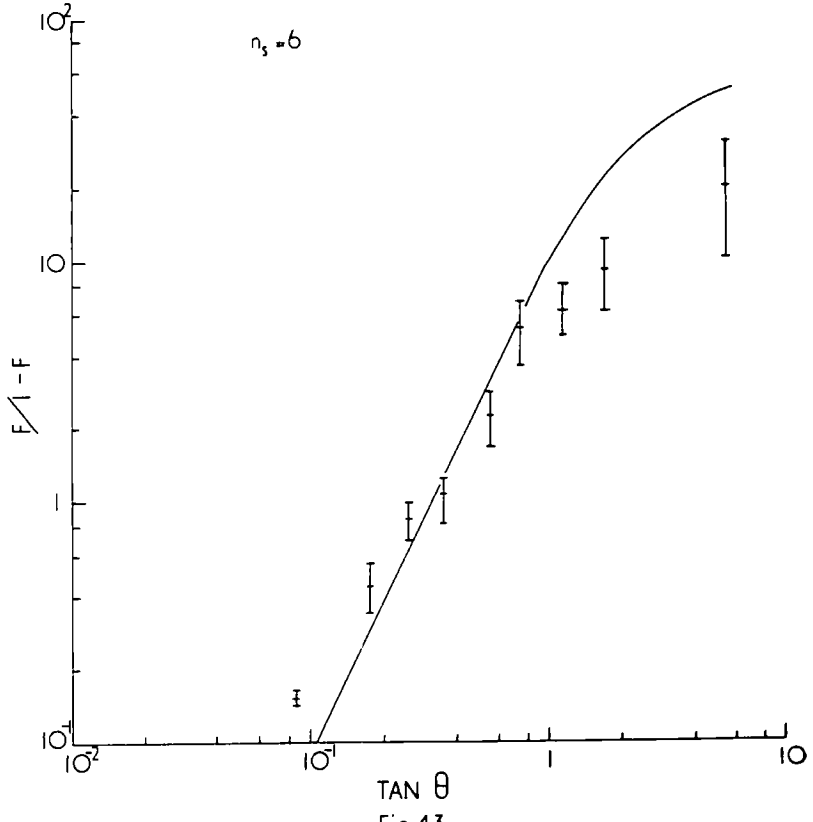
$n_s = 6$
10^2
10
1
10^{-1}
F/1 - F
10^{-2}
10^{-1}
1
10
TAN θ
Fig.43.

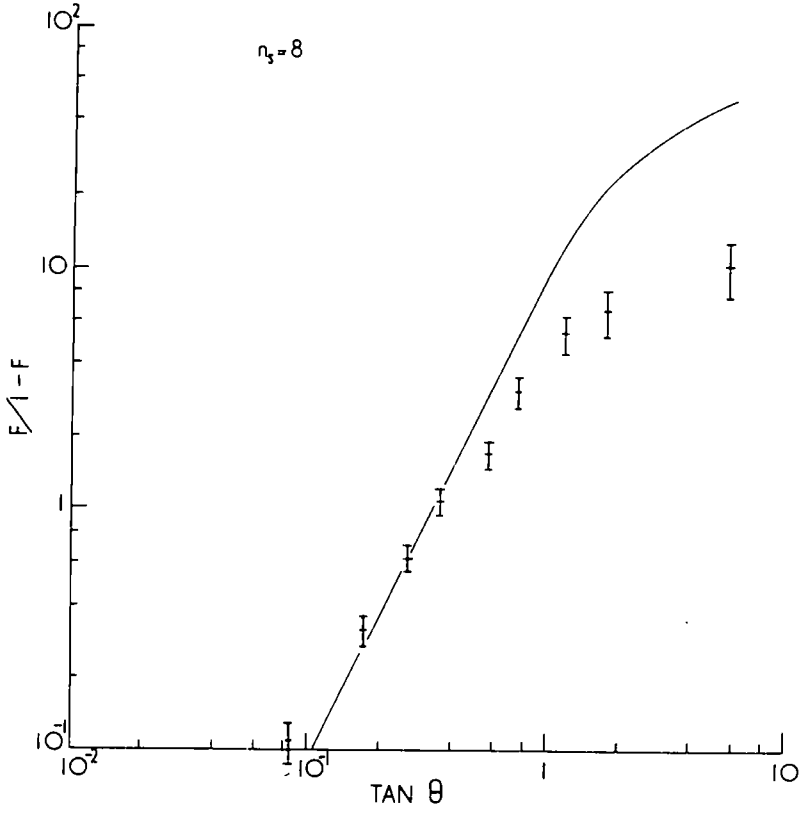
$n_s = 8$
10^2
10
1
10^{-1}
10^{-2}
10^{-1}
1
10
F/1 - F
TAN θ
Fig.45.

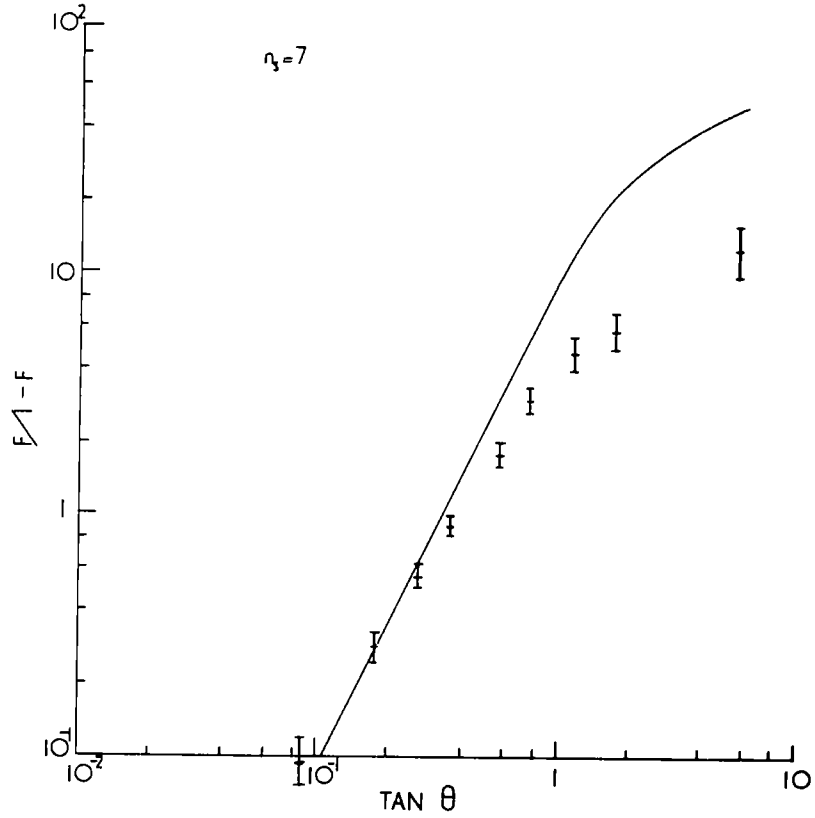
$n_s = 7$
10^2
10
1
10^{-1}
10^{-2}
10^{-1}
1
10
F/1 - F
TAN θ
Fig.44.

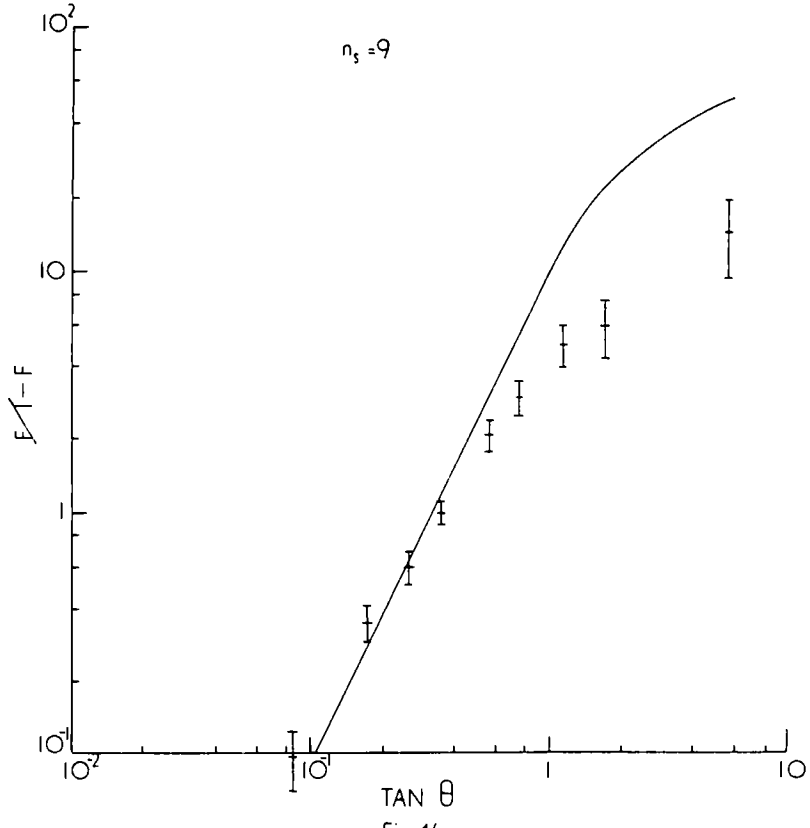
$n_s = 9$
10^2
10
1
10^{-1}
10^{-2}
10^{-1}
1
10
E/1-F
TAN θ
Fig.46.

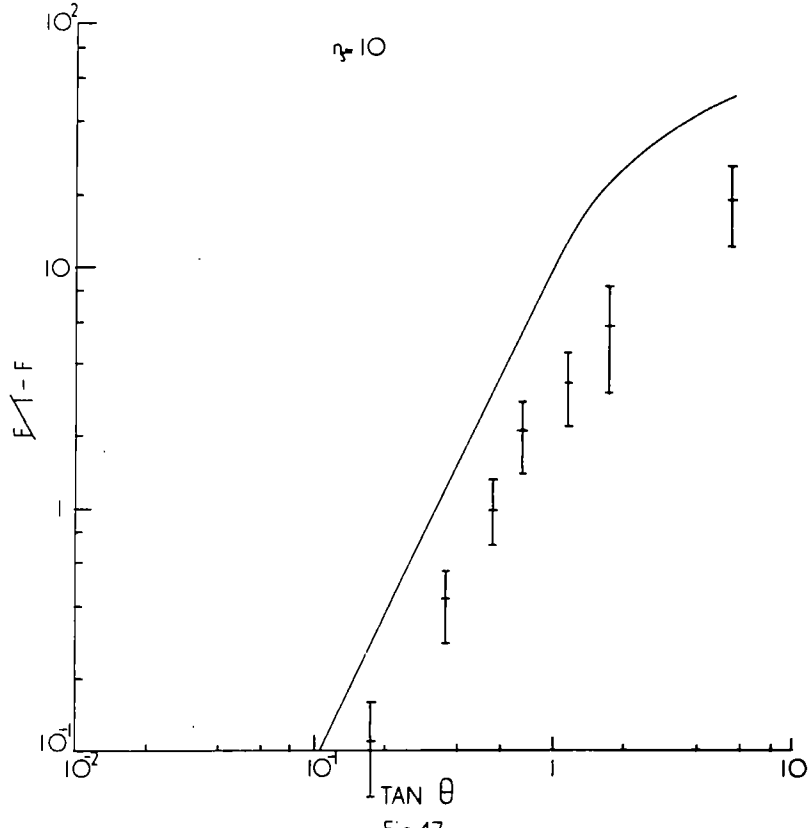
$n_s = 10$
10^2
10
1
10^{-1}
10^{-2}
10^{-1}
1
10
E/1-F
TAN θ
Fig.47.

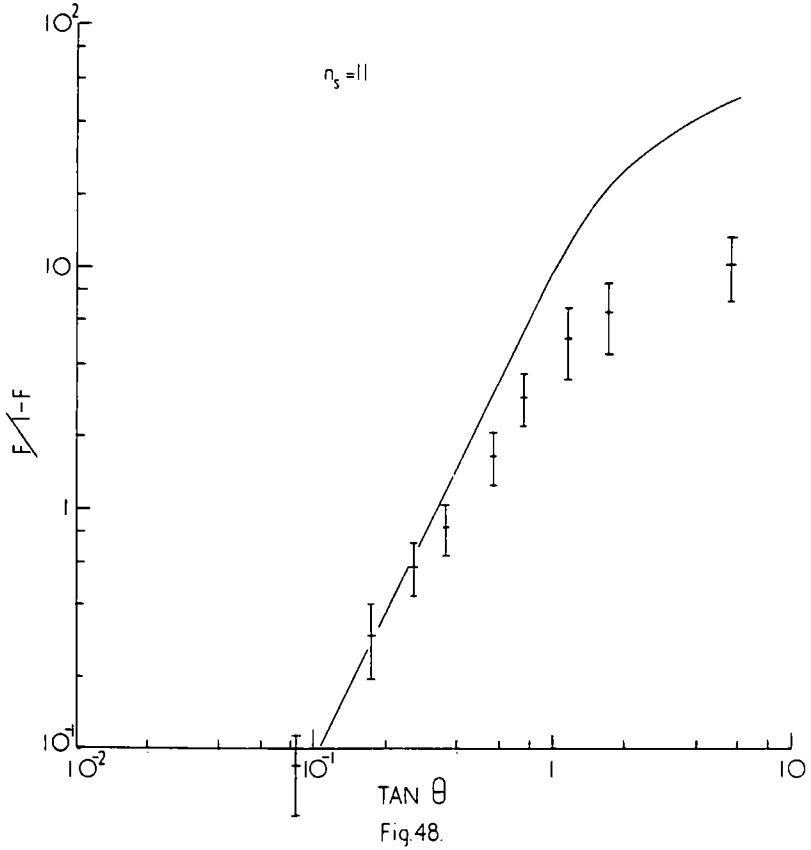
$n_s = 11$
10^2
10
1
10^{-1}
10^{-2}
10^{-1}
1
10
E/1-F
TAN θ
Fig.48.

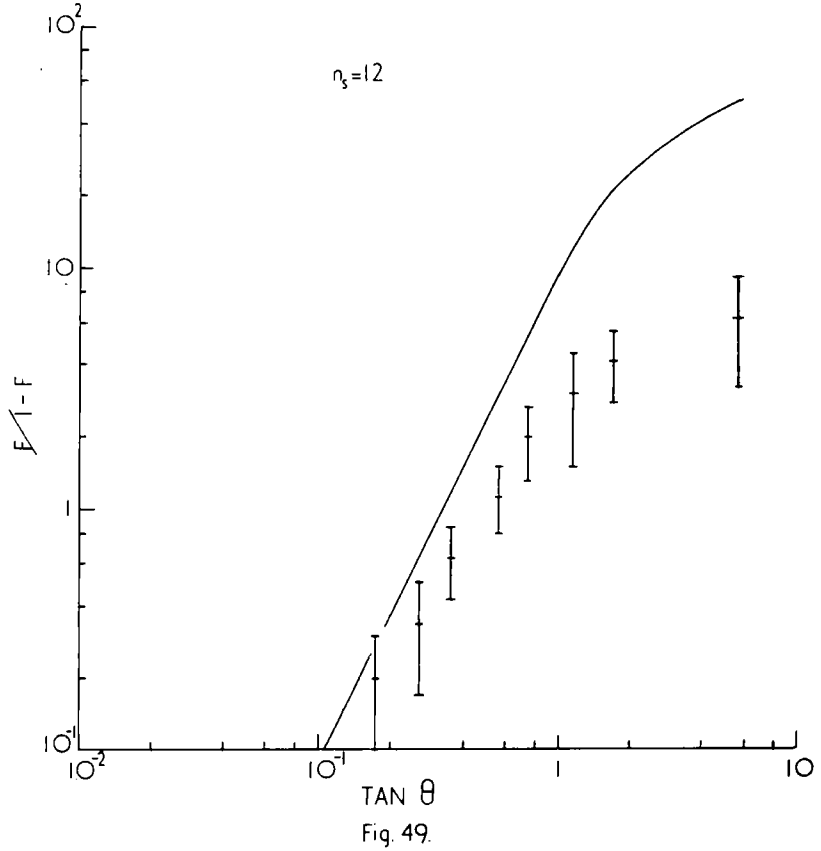
$n_s = 12$
10^2
10
1
10^{-1}
10^{-2}
10^{-1}
1
10
E/1-F
TAN θ
Fig. 49.

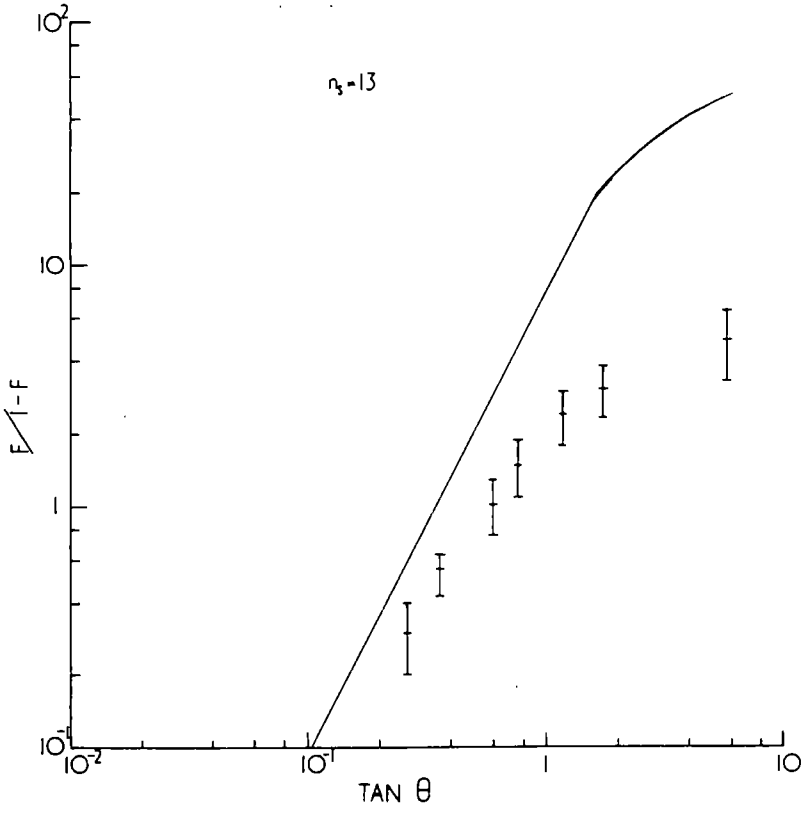
n_3=13
10^2
10
1
10^{-1}
E/1-F
10^{-2}
10^{-1}
1
10
TAN θ

Fig. 50

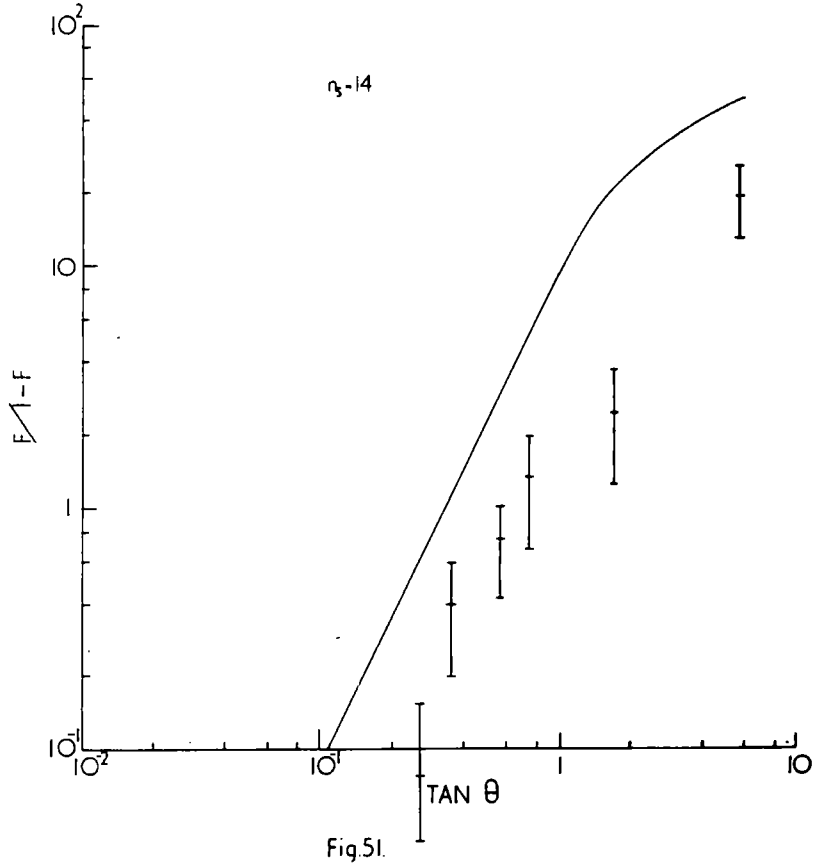
n_3=14
10^2
10
1
10^{-1}
E/1-F
10^{-2}
10^{-1}
1
10
TAN θ

Fig. 51.

APPENDIX A.4.

Calculation of the average Potential Path Length in Nuclear Matter Secondary Particles Produced by 16.3 GeV π^--mesons in the Nuclei of Ilford G.5 Emulsion

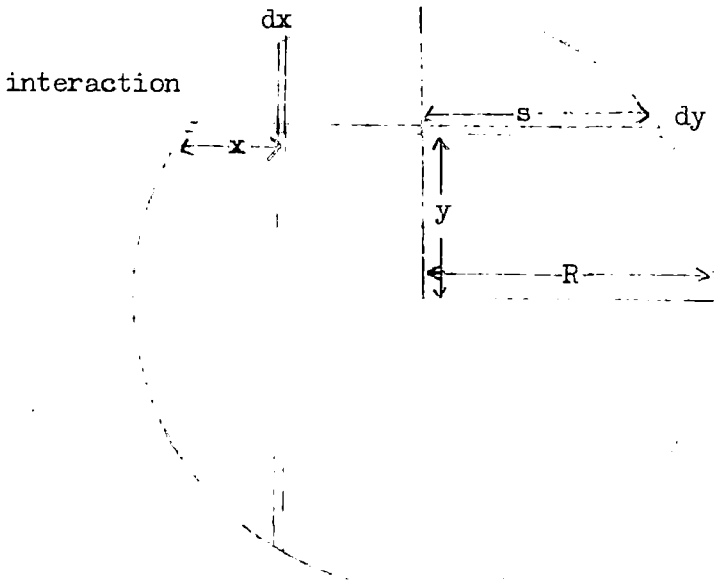

The secondary particles are assumed to travel in the forward direction.

The average potential path length $\bar{\ell}$ is given by

$$\bar{\ell} = \frac{\Sigma \text{ potential length}}{\text{nos. of produced } \pi\text{-mesons}}$$

$$\bar{\ell} = \frac{\int_{s=0}^{R} \int_{x=0}^{2s} \frac{2ydy}{R^2} \cdot e^{-x/\lambda} \cdot \frac{dx}{\lambda} \, n_\pi (2s-x)}{\int_{s=0}^{R} \int_{x=0}^{2s} \frac{2ydy}{R^2} \cdot e^{-x/\lambda} \cdot \frac{dx}{\lambda} \cdot n_\pi}$$

This reduces to

$$\bar{\ell} = \frac{4}{3} R \left\{ 1 - \frac{\lambda}{R} e^{-2R/\lambda} + \frac{\lambda^2}{2R^2} (1-e^{-2R/\lambda}) \right\}^{-1} - \lambda$$

\+ −

where R is the radius of the nucleus concerned and λ the mean free path in nuclear matter for 16.3 GeV mesons. A table of values of G.5 emulsion is given below:-

Nucleus	I	Ag	Br	S	O	N	C
$\bar{\ell}$ in fermis	5.16	4.71	3.93	1.77	0.63	0.39	0.19

The weighted mean of the values of $\bar{\ell}$ is given by $\Sigma N_i R_i^2 \bar{\ell}_i / \Sigma N_i R_i^2$ and is 3 fermis.

PUBLICATIONS BY THE AUTHOR

The interactions of π^--mesons with complex nuclei in the energy range (100-800) MeV Part III.

Interaction lengths and diffraction scattering of 300 MeV π^--mesons in G5 emulsion.

1962, Phil. Mag., 7, 237, (with J.V. Major and P.G.J.T. Parkhouse).